


**REVIEW**

# Recent developments in data acquisition, treatment and analysis with ion mobility-mass spectrometry for lipidomics

María Moran-Garrido<sup>1</sup> | Sandra. M. Camunas-Alberca<sup>1</sup> | Alberto Gil-de-la Fuente<sup>1,2</sup> | Antonio Mariscal<sup>1,2</sup> | Ana Gradillas<sup>1</sup> | Coral Barbas<sup>1</sup>  | Jorge Sáiz<sup>1</sup>

<sup>1</sup>Centre for Metabolomics and Bioanalysis (CEMBIO), Departamento de Química y Bioquímica, Facultad de Farmacia, Universidad San Pablo-CEU, CEU Universities, Urbanización Montepríncipe, Madrid, Spain

<sup>2</sup>Departamento de Tecnologías de la Información, Escuela Politécnica Superior, Universidad San Pablo-CEU, CEU Universities, Urbanización Montepríncipe, Madrid, Spain

**Correspondence**

Jorge Sáiz and Coral Barbas, Centre for Metabolomics and Bioanalysis (CEMBIO), Departamento de Química y Bioquímica, Facultad de Farmacia, Universidad San Pablo-CEU, CEU Universities, Urbanización Montepríncipe, 28660, Boadilla del Monte, Madrid, Spain.

Email: [jorge.saizgalindo@ceu.es](mailto:jorge.saizgalindo@ceu.es); [cbarbas@ceu.es](mailto:cbarbas@ceu.es)

**Abstract**

Lipids are involved in many biological processes and their study is constantly increasing. To identify a lipid among thousand requires of reliable methods and techniques. Ion Mobility (IM) can be coupled with Mass Spectrometry (MS) to increase analytical selectivity in lipid analysis of lipids. IM-MS has experienced an enormous development in several aspects, including instrumentation, sensitivity, amount of information collected and lipid identification capabilities. This review summarizes the latest developments in IM-MS analyses for lipidomics and focuses on the current acquisition modes in IM-MS, the approaches for the pre-treatment of the acquired data and the subsequent data analysis. Methods and tools for the calculation of Collision Cross Section (CCS) values of analytes are also reviewed. CCS values are commonly studied to support the identification of lipids, providing a quasi-orthogonal property that increases the confidence level in the annotation of compounds and can be matched in CCS databases. The information contained in this review might be of help to new users of IM-MS to decide the adequate instrumentation and software to perform IM-MS experiments for lipid analyses, but also for other experienced researchers that can reconsider their routines and protocols.

**KEYWORDS**

acquisition, data, databases, ion mobility, lipidomics, mass spectrometry

## 1 | INTRODUCTION

In recent years there have been several advances in lipidomic analyses because of the great difficulty of lipid characterization given their

overwhelming complexity and structural heterogeneity [1, 2]. One of the recent innovations to deepen expertise about them has been the coupling of ion mobility (IM), a chromatographic technique, typically liquid chromatography (LC), and mass spectrometry (MS), providing a third dimension of separation that has been demonstrated to improve the confidence level in lipid identification [3–6]. Furthermore, IM has provided the possibility of separating isomers that previously were not able to be measured separately [7–10]. It works by separating ions in the gas phase according to their mobilities in a way that bigger and more extended ions reach the detector at different times than the smaller and more compact ones. Many IM instruments allow for

**Abbreviations:** IM, Ion mobility; MS, Mass spectrometry; CCS, Collision cross section; LC, Liquid chromatography; DTIMS, Drift tube IM; TWIMS, Travelling Wave IM; SLIM, Structures for lossless ion manipulation; cIM, Cyclic TWIMS; TIMS, Trapped IM; FAIMS, Field asymmetric waveform IM; DMS, Differential mobility spectrometry; CV, Compensation voltages; Ec, Compensation field; PRS, Pseudo-random pulsing sequence; DDA, data-dependent acquisition; DIA, data-independent acquisition; Q-BBI, Quadrupole broad band isolation; QRAI, Quadrupole resolved all ions; CTS, Concerted tandem; TAP, Time-aligned parallel fragmentation; PC, Phosphatidylcholine; PASEF, Parallel accumulation-serial fragmentation.

This is an open access article under the terms of the [Creative Commons Attribution-NonCommercial-NoDerivs](https://creativecommons.org/licenses/by-nc-nd/4.0/) License, which permits use and distribution in any medium, provided the original work is properly cited, the use is non-commercial and no modifications or adaptations are made.

© 2022 The Authors. Proteomics published by Wiley-VCH GmbH.

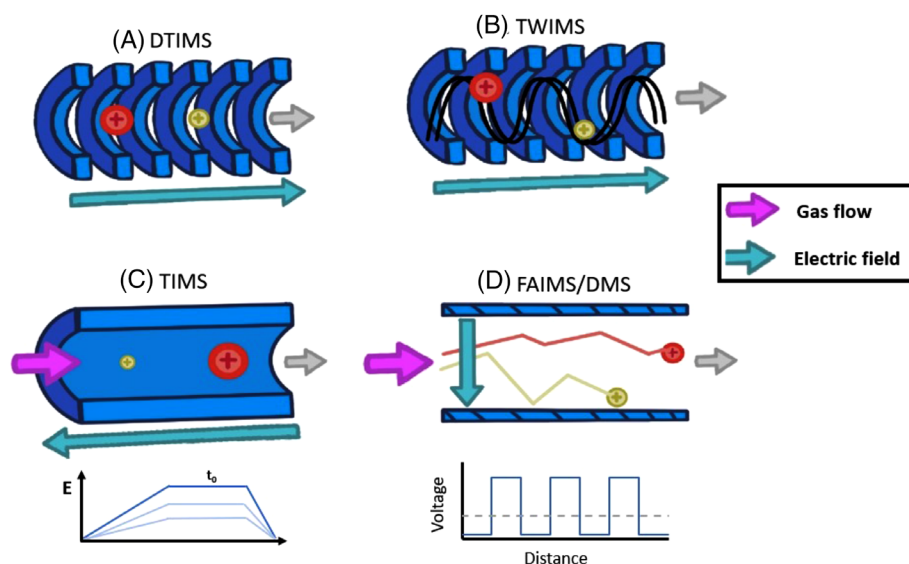


**FIGURE 1** Schematic representation of commercially available IM analyzers. (A) DTIMS, (B) TWIMS, (C) TIMS, (D) FAIMS or DMS.

the calculation of the cross-section (CCS), an instrument independent physical property of ions that measures the shape and the size of the molecules, which can be used to increase the confidence on compound identification and in the creation of libraries [11, 12].

There are different commercially available IM-MS systems whose main principles have been thoroughly covered in specific reviews [11, 13–15]. As an overview, current IM instrumentation can be divided into three types: time-dispersive; confinement and selective release; and space-dispersive [11].

**Time-dispersive:** In which ions travel through the same path and reach the detector at different times. The main common time-dispersive instruments are Drift Tube IM (DTIMS) and Travelling Wave IMS (TWIMS) (Figure 1A,B). DTIMS consists of several ring electrodes stacked alongside each other filled with an inert static gas through which ions move directed by a uniform electric field. This is the only system in which CCS can be directly calculated from the arrival times via the stepped-field method. TWIMS has a similar configuration to DTIMS, but it works with a non-uniform electric field creating voltage waves that move the ions along the IM cell. Another difference in practice between TWIMS and DTIMS is that the CCS cannot be obtained directly by TWIMS instrumentation as DTIMS does. Then to calculate the CCS in TWIMS of the analytes in sample, it is necessary the calibration using compounds with known CCS, which, at the same time, must be structurally similar calibrants (refer to section *CCS calculation* for more details). Time-dispersive is the most common type of separation for untargeted lipidomics, as it permits the analysis of all the ions present in a sample. Nonetheless, it has relatively low resolving power compared to other systems, which limits the detection of low-intensity signals and the separation of isomers [14, 16–19]. To increase resolving power, new systems based on TWIMS have been developed, in which drift paths are greatly increased to promote collisions with the buffer gas and improve ion separation. These are structures for lossless ion manipulations (SLIM) which are reduced printed circuit with up to 13 m total length path [20]. Another alternative is the cyclic TWIMS (cIM),

which enhances resolution by performing several ion passes through the closed-loop drift cell included in the instrument [21]. DTIMS instruments are typically attached to Q-TOF instruments, such as the 6560 from Agilent Technologies or the SYNAPT XS and the Cyclic series from Waters.

**Confinement and selective release** in which ions are trapped by an electric field as they are pushed forward by a moving buffer gas. By decreasing the electric field, they are selectively released in a contrary manner to time-dispersive, so ions of bigger size and smaller mobility are eluted first. Trapped Ion Mobility Spectrometry (TIMS) is the main confinement and selective release instrument (Figure 1C). It is very selective and has a higher resolving power than time-dispersive instrumentation which makes it a great candidate for isomer separation. However, changes in the conditions, such as shorter trapping times, for a more untargeted approach can be made. Just as in TWIMS, CCS cannot be determined directly except if a calibration is performed [22, 23]. As in DTIMS, the typical setup for TWIMS includes an LC separation before the IM and a Q-TOF after.

**Space-dispersive** in which ions are pushed by a buffer gas, traveling through different paths as high and low electric fields are applied between two electrodes. It acts as a mobility filter where a specific compensation voltage is applied to guide an ion of a particular mobility to the detector whilst all the other ions are lost. In this group, we can find Field Asymmetric Waveform Ion Mobility Spectrometry (FAIMS), otherwise known as Differential Mobility Spectrometry (DMS) (Figure 1D). Because of the use of high and low voltages, CCS cannot be determined, rather, compensation voltages (CV) or compensation field ( $E_c$ ) are used as mobility descriptor [9, 24]. However, a recent approach for the CCS calculation has been developed, which is discussed in the CCS calculation section, below. This type of separation is very selective, it highly reduces chemical noise, and it has a very high resolving power, so it is the most useful for isomer separation. However, it is not the most suitable for untargeted lipidomics, as only ions of a specific mobility are analyzed at a time [25]. For this reason, Q-TOFs

in FAIMS are usually avoided, being the triple quadrupoles or Orbitraps the detectors of choice for space-dispersive IM.

Some of the benefits of using IM-MS over MS-only include increased peak capacity and separation power of isomers and isobars, reduction of chemical noise, a superior quality spectra acquisition and a higher confidence level of identification by including the CCS as a quasi-orthogonal property [3, 26–28]. Nonetheless, there are some limitations, like low duty cycles and relatively low resolving power, mainly in time-dispersive instrumentation [29]. Additionally, the great complexity and large amounts of generated data remarkably reduce the possible software available for data treatment and analysis, as well as significantly increase the necessary computer requirements and the processing time [30–32]. The review discusses on the current instrumentation and the newest alternatives for treatment and analysis of data. We focus on commercial instruments and free software, since these are the available options for the general IM-MS user. We also discuss on the added value of the CCS value for lipid identification, including the different CCS databases and software available for identification purposes that are currently available and have recently been developed. Besides, we expect this review can be of help and guide for the IM-MS analysts, helping them in the decision-making process in lipidomic workflows.

## 2 | DATA ACQUISITION

As part of an analytical technique containing an MS stage, an IM-MS instrument can be operated in the common MS modes: scan and MS/MS modes with electrospray ionization as the most common ionization source used either in positive or negative mode. In the scan ions of an  $m/z$  range transverse the IM reaching the detector while in MS/MS mode some selected ions are fragmented in a collision cell, reaching the detector all their products or some selected ones. In this section, we focus on the different acquisition modes in IM-MS, which might entail significant differences due to the existence of the IM stage compared to the equivalent analysis in MS. The advantages and disadvantages of those approaches are also discussed.

### 2.1 | Scan mode

This mode permits to monitor ions in a desired mass range. It is used to obtain a broad view of the composition of a sample, as the system will record abundances and arrival times for all measured  $m/z$  values. Typically used in untargeted approaches, scan analyses will result in large, datasets composed of many unknown features, which makes the interpretation of the data a complicated task.

The fact that only a small proportion of the ions generated in the ion source can enter the IM, while all the others are lost, affects the sensitivity of the analysis, reducing the ions that are effectively used in the acquisition, or duty cycle. Using a trapping cell before the IM stage in which ions are accumulated and released, is a partial solution [33]. This will increase the number of ions reaching the detector, thus increasing

duty cycle, but it can affect quantitation of low  $m/z$  ions and result in detector saturation, especially with increasing trapping times [34]. An alternative is to split the ion packets into smaller ones that are pulsed into the IM, reducing the ion losses, and reaching up to 50% increase in duty cycle [35]. This is known as multiplexing the IM signal in time (temporal multiplexing) and can be performed in pulsed time dispersive IM, such as DTIMS and TWIMS. Multiplexing has shown important advantages compared to single pulse acquisition modes. Ions are trapped for shorter times in the trap cell than in single pulse IM and they are released in a *pseudo*-random pulsing sequence (PRS). A multiplexed analysis results in as many signals as ion packets are pulsed in the PRS. For example, in a 4-bit PRS, when an ion is visualized in an abundance map showing  $m/z$  and the arrival time, eight signals will be shown at different arrival times following the random pulsing pattern (Figure 2). However, for CCS calculation and data interpretation, data must be combined and deconvoluted by tracing back the pattern used in the PRS using specific software [34, 36].

The advantages of a multiplexed over single pulse analysis have been extensively covered in proteomics analysis and include noise reduction, increased sensitivity, lower probability of peak saturation, extended working linear ranges and increased duty cycle [33, 35, 36]. For amino acids and other metabolites, Causton et al. [34] demonstrated that when performing a 4-bit multiplexing analysis of a yeast extract, there was 9-fold sensitivity increase and an evident noise reduction over the single-pulse mode with the same trapping times, in particular for  $m/z$  below 250. Most recently, an evaluation of the effects on lipid analysis of different trapping times in single pulse and multiplexed modes was performed by da Silva et al. [37]. Results from high trapping times were concordant with previous findings for other molecules, in which high trapping times increased signal intensity and duty cycle at the expense of possible detector saturation. On the other hand, in multiplexing mode, different trapping times did not significantly change sensitivity, especially for lipids of  $m/z$  over 300. Moreover, it was found that divergent sensitivities using the aforementioned modes appear to be influenced by the lipid structure, as multiplexing mode increased sensitivity in fatty acids, but single pulse did so in carnitines. Surprisingly, when making the same comparison in complex samples like HepaRG cell extracts, there was no signal intensity gain for most lipids in multiplexing mode. Nonetheless, lipidomics analysis in complex samples can still benefit from multiplexing in means of detector saturation and noise reduction that can increase peak deconvolution, feature finding and as a result provide a more confident lipid annotation, especially of low abundant lipids such as oxylipins [37].

### 2.2 | MS/MS fragmentation mode

MS/MS analyses are widely used, providing essential information for structural elucidation and lipid identification [38, 39]. MS/MS analyses can be categorized into two groups: targeted and untargeted. In targeted MS/MS, a list of ions of interest is created by the user and the system filters those masses being subsequently fragmented. Untargeted approaches do not need prior knowledge about the sample

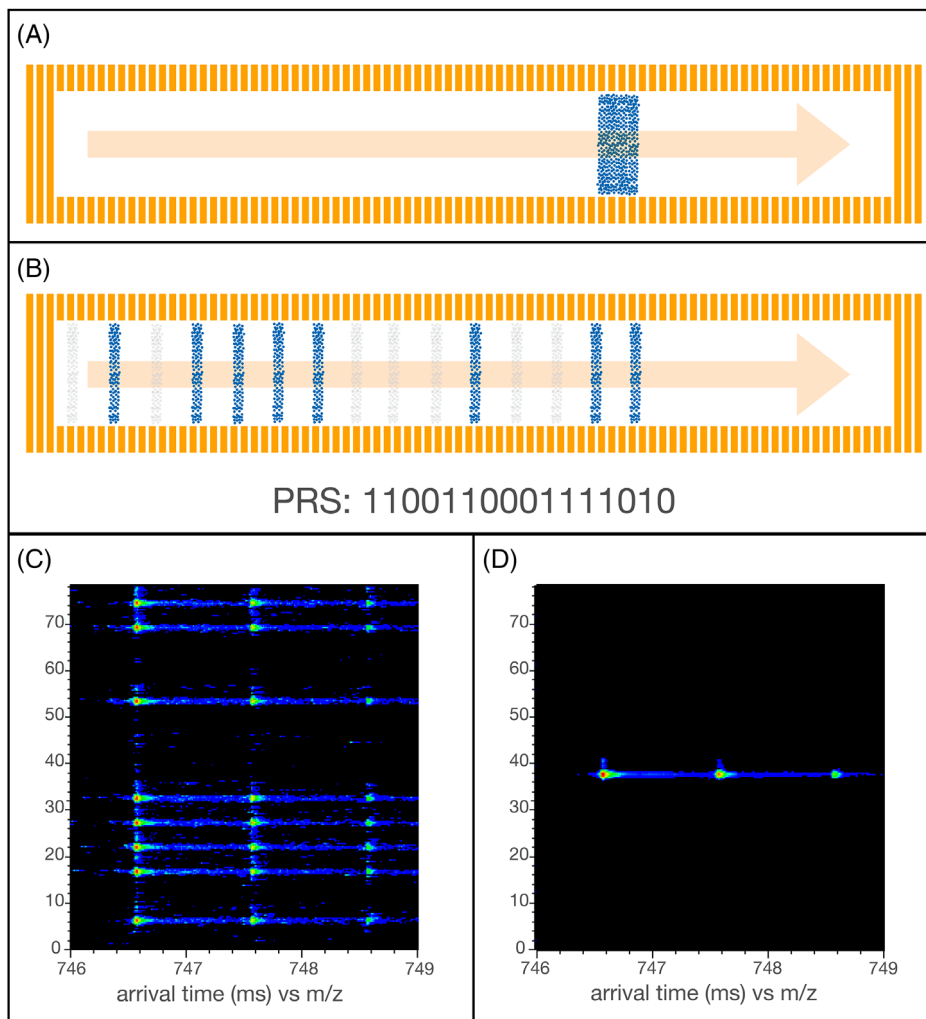


**FIGURE 2** (A) Representation of a single pulse in IM, in which ions are pulsed from left to right, towards the detector. (B) Representation of a PRS. The eight blue bands represent the eight ion packets pulsed, with the ion gate open (1), while the blurred bands represent events in which ions are not released (0). Higher trapping times in single pulsed IM compared to multiplexed IM are represented by a wider band of ions. (C) Result of a 4-bit multiplexed analysis for a  $m/z$  in which the eight packets can be observed along 70 ms following a PRS. (D) Same data after demultiplexing in which all the packets are combined by software in one having a single arrival time, around 38 ms.

composition and ions will be fragmented in data-dependent acquisition (DDA) or data-independent acquisition (DIA) modes [40]. Including IM separation before MS/MS analyses has shown advantages based on the extra separation, such as background noise reduction and consequently more reliable spectra interpretation, which improves the sensitivity in the analysis of lipid mixtures. Moreover, the quadrupoles used for MS/MS analysis have much less resolution than a TOF and artifacts are commonly introduced into the collision cells. IM can filter these artifacts according to the arrival times, providing cleaner MS/MS spectra that are free of interference and enhances its interpretation [26, 28, 40, 41]. Figure 3 shows the differences of the MS/MS spectra when incorporating IM to the analysis regarding the same spectra using LC-MS/MS.

- In DDA analysis, two types of analyses are performed consecutively. First, in an IM scan, the most abundant ions are selected by the software. Then, in a second analysis, those ions are iso-

lated one by one by the quadrupole and successively fragmented to obtain the MS/MS spectra. While DDA is an automated process, the main disadvantage is the repeated fragmentation information that generates. For example, if various lipids coelute showing different intensities, only those with higher intensity will be selected and recurrently fragmented. This is reflected as a low coverage of analytes compared to other approaches. To avoid this, iterative analysis of a sample can be performed [42]. For this, the sample is injected multiple times and the ions selected in one scan are excluded from the subsequent ones (Figure 4). However, as far as we know, iterative analysis has not been introduced in IM-MS/MS analysis so far. Alternatively, manual exclusion lists should be created, as done by Pezzatti et al. [43], in which the fragmented ions from the first analysis were manually excluded in a second analysis, increasing the number of covered analytes by 20%–25% of all annotated metabolites. However, the creation of manual lists is highly time-consuming and might not be so effective in increasing the analyte coverage,

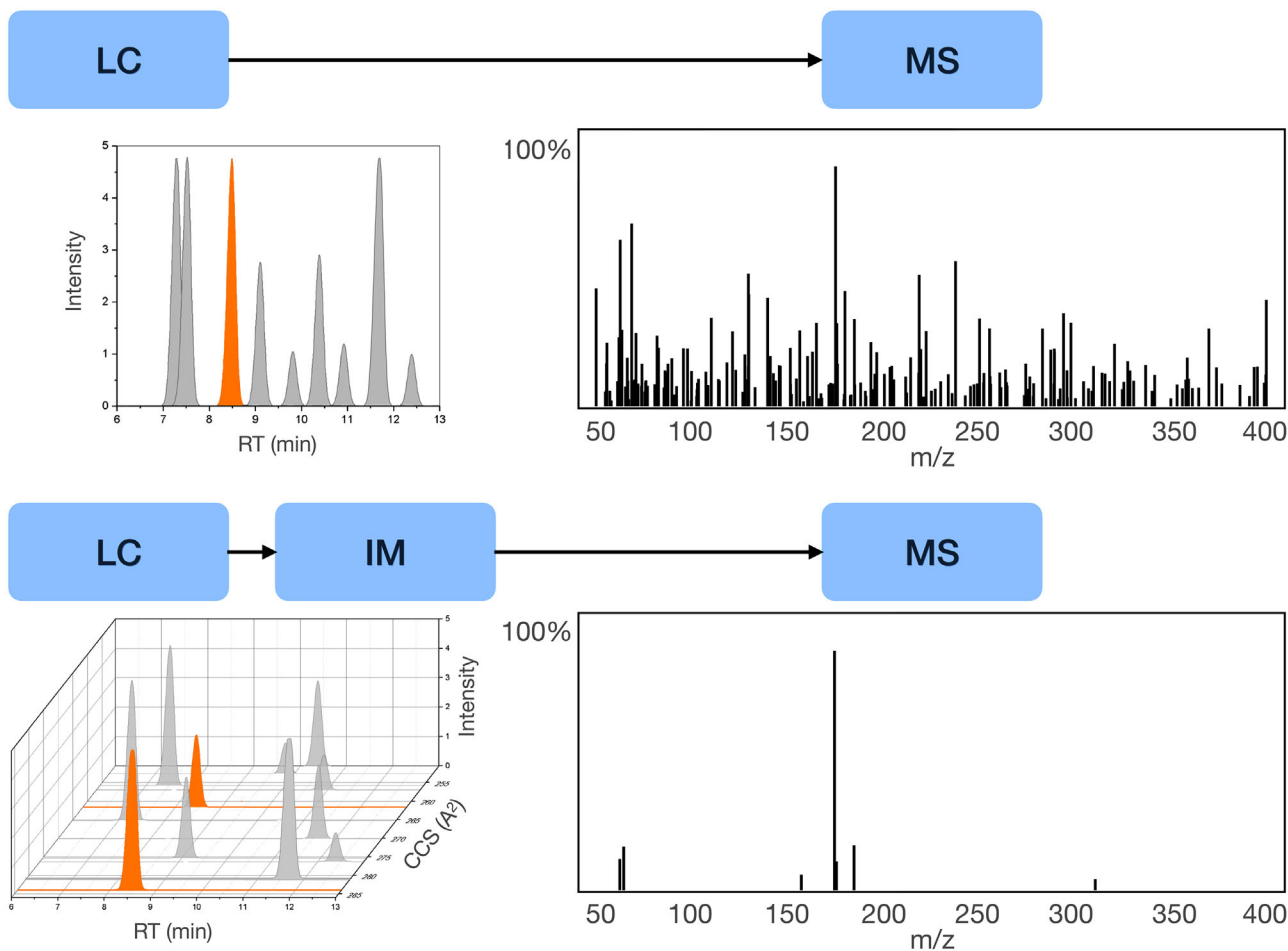


**FIGURE 3** In LC-MS, the separation of metabolites using a second separation technique cleans the acquired MS/MS spectra from artifacts previously co-eluting in the chromatographic column, thus easing its interpretation and resulting in a higher confidence level of the metabolite identification.

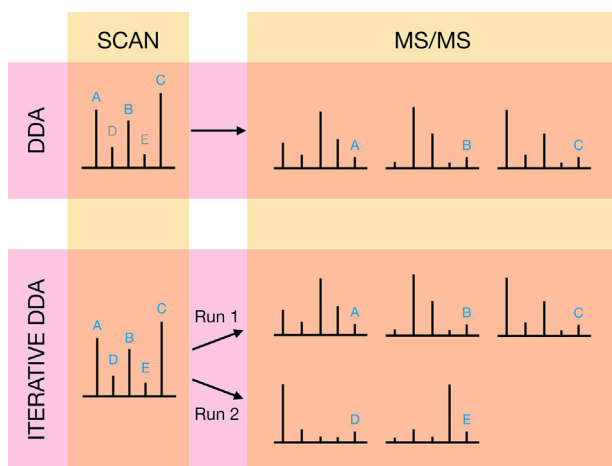


**FIGURE 4** Comparison of DDA and iterative DDA. In DDA, only the most intense ions (A, B, and C), while the less abundant (D and E) are not fragmented. In iterative DDA, A, B and C can be manually excluded in IM after the first run and D and E are fragmented in the second one.

when compared with DIA analyses. This and the fact that not all vendors offer the possibility of DDA-IM analysis might explain why DIA seems to be the preferred untargeted MS/MS mode in IM.

- In DIA analysis ions are fragmented without any previous selection. It is more frequently used in untargeted workflows than DDA due to its wider coverage of analytes and its availability. DIA also executes two consecutive types of analysis, alternating low and high collision energies. In the first analysis all the ions are transferred to the detector without fragmentation (low collision energy) while in the next one, fragmentation occurs (high collision energy) at fixed energy. To achieve this, the quadrupole does not filter any masses, acting just as an ion guide. Therefore, assigning product ions to their precursors is not as straightforward as in DDA, as multiple precursors are fragmented at the same time. This has been considered the main disadvantage attributed to DIA [43]. But, when IM separation happens before fragmentation, precursor and product ions can be aligned according to their mobility behavior, helping in the product-precursor assignment (Figure 5). However, data might require IM time alignment since precursor and product might show different mobilities due to the induced energy applied during the fragmenta-

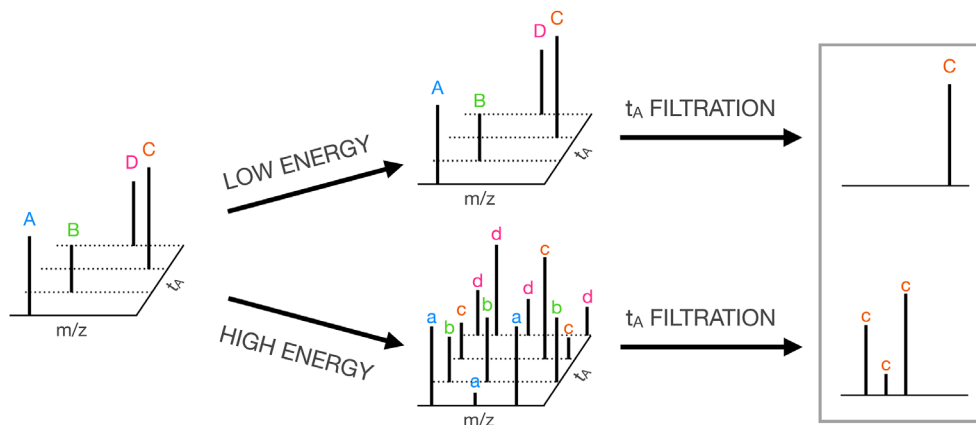


**FIGURE 5** Representation of a DIA analysis in which low energy and high energy fragmentation are performed for all ions generated in the ion source. Matching precursors and products is possible thanks to the IM information, which is the same for both. t<sub>A</sub>: Arrival Time.

tion [44]. Even more, if coeluting isomers and isobaric forms have different mobility behavior, their product ions can be discriminated, like it was done by Hellhake et al. [45] with two isomeric oxylipins in human plasma. The fact that a fixed energy is used for the fragmentation on DIA is another disadvantage in these analyses, since the fragmentation cannot be adjusted for each molecule, which often results in poor fragmentation spectra, when the energy is not enough to fragment the ion.

DIA in IM has been successfully used for the identification of lipids in different studies. Like Hinz et al. [46] to study the formation of different adducts and clusters in oxylipin standards in human platelets or Hines et al. [28] to identify different lipids in *Escherichia coli* samples.

Besides, the integration of IM before the collision cell permits the elimination of in-source fragmentations and therefore cleaning of the MS/MS spectrum. These fragments that commonly occur in lipids, are introduced in the IM and reach the detector since the quadrupole is not working in DIA. Eliminating them, by drift time filtration, has provided more accurate annotations in DIA with IM. Although a higher number of rightly annotated compounds was obtained, many signals were lost when comparing to an analysis without IM due to the decreased sensitivity in these analyses. This was seen by Pezzatti et al. [43] in human plasma samples when analyzing the whole metabolome, including lipids and by Plachaka et al. [47] in human urine samples when analyzing steroid doping agents. Most recently, thanks to the drift time filtration in DIA-IM, Kirkwood et al. [48], created an accurate lipid library with clean fragmentation spectra from human plasma samples without the need of standards. This was later used by Odenkirk et al. [49] for lipid identification in brain samples.

There are some exceptions in DIA in which not the whole ion population is fragmented. They can be categorized by IM type:

- *Q-BBI and Q-RAI in DTIMS*: New and improved instrumentation is being developed in DTIMS to include the quadrupole selection after the IM separation in DIA workflows, improving the acquisition efficiency and the clarity of the obtained spectra. Two simi-

lar approaches have been made so far: a prototype Ion Mobility directed Quadrupole Broad Band Isolation (IM-Q-BBI) and an Ion Mobility Quadrupole Resolved All Ions (IM-Q-RAI). In IM-Q-BBI [50], the quadrupole isolation window (the  $m/z$  range) is correlated with the mobility of the ions. In other words, the window is quickly ramped up to fit with the increasing drift times of the precursor ions in one IM event. To perform IM-Q-BBI a few optimizations must be done before the analysis to properly correlate the mobility of ions and the quadrupole selection. IM-Q-RAI [51] uses a wide isolation window (up to 100 Da), which is ramped in a timeframe of one millisecond. Considering that the correlation of mobility and mass in lipids has been demonstrated [52, 53], the application of these approaches to lipidomic analyses is very well-suited since it permits lipid class identification. Both approaches resulted in the removal of unwanted interferences in the MS/MS spectrum at higher levels than a regular DIA-IM analysis, therefore enhancing the annotations' confidence level. Another advantage is the higher efficiency of the mass analysis in the quadrupole analyzer, which increases the duty cycle. Also, these approaches have been associated to improve the linearity and a higher number of working ranges. As a drawback, they cannot be combined with multiplexing, since the IM is used in different ways, losing all the advantages of the multiplexed operation.

- *CTS and TAP in TWIMS*: TWIMS in Synapt systems from Waters permits alternative fragmentation approaches that provide valuable information that can be useful for metabolite annotation. The following approaches use a first stage of quadrupole filtering for product fragmentation and IM separation of the products. The fact that a quadrupole is used in a first instance permits targeted MS/MS and nontargeted DIA analysis. The utility of Concerted Tandem (CTS) analysis has been demonstrated in the identification of lipids based on the unique mobility of the product ions and their exact mass in complex mixtures [54–56]. Time-Aligned Parallel Fragmentation (TAP) performs two fragmentations: a first one before IM separation and a second one after it. This provides first and second-generation fragment ions that are aligned based on drift

time, enhancing the structural information of analytes [57]. It has been used for the localization of fatty acyl and double bond position in phosphatidylcholines (PC) in plasma samples [57] and to provide information on the *cis/trans* geometry of the double bonds [58].

- **PASEF in TIMS:** In a conventional TIMS-MS/MS analysis, the quadrupole selects just one  $m/z$  for its fragmentation in each TIMS separation, whilst all the other ions that continue to elute are not fragmented, losing and estimated 90% of the acquisition efficiency [42, 59]. To improve the acquisition efficiency, Parallel Accumulation–Serial Fragmentation (PASEF) was developed by Meier et al. [59] and it was later included in timsTOF Pro by Bruker Daltonics [60]. In PASEF, the quadrupole is set to isolate as many precursors as possible by changing the selected  $m/z$  for each ion that elutes from TIMS, greatly increasing the number of precursors selected and the fragmentation information provided [60]. Besides, DDA-PASEF can be operated in iterative mode, covering even more precursor ions [42]. The performance of PASEF in lipidomics was evaluated by Vasilopoulou et al. [42] in human plasma, mouse liver tissue and HeLa cells samples. The use of PASEF increased the number of fragmented features 11.5 times compared to standard TIMS-MS/MS, with an average of 15 fragmented precursors per PASEF scan. The number of identified lipids augmented more than 3 times, establishing PASEF as a great tool for high coverage lipidomics. Most recently PASEF was used for the identification on chain level of lipids in spleen tissue. This permitted to characterize not just nonisomeric lipids, but to identify two coeluting glycerophosphoglycerols (PG), PG(18:1\_18:2) and PG(16:0\_20:3), that otherwise would not have been distinguished, by providing a CCS-filtered fragmentation spectra [61]. This approach is a DDA mode, but diaPASEF has been implemented as well. For it, a quadrupole  $m/z$  isolation window is used which, based on the mobility of the ions, is automatically adjusted. This method has shown promising results in proteomics but is yet to be used in lipids [62].

It can be inferred from the available working modes in IM that different approaches for sample analysis are currently available. Some of them are relatively complementary (DDA and DIA) while some others are exclusionary (e.g., multiplexing IM-QRIA is not possible). Each approach has its own characteristics resulting in particular advantages and disadvantages in metabolite identification and structural elucidation. To make the most of IM-MS/MS, combined DDA and DIA analysis is suggested. By combining both analyses, a higher coverage of the lipidome is potentially achieved [40]. A hybrid DDA and DIA has recently been reported utilizing a Vion IM-QTOF, with a full IM scan, DIA-IM of all precursors and DDA-IM of the most abundant precursors [63]. This approach improved peak capacity, selectivity, and resolution of coeluting compounds, along with higher quality spectrum, higher coverage of analytes and faster structural elucidation. It is important to highlight that most of the lipidomics approaches are done with a previous LC separation, which provides additional information about the analytes as RT data. This supports the identification of some analytes, including lipid isomers, while increases the amount and complexity of the generated data. Much more information can

be extracted from a combined approach (LC-DIA-DDA-IM-MS/MS), resulting also in a higher amount of data that hinders its interpretation. Manual analysis and inspection of all the generated data are therefore unfeasible. Moreover, the fact that many of these working modes have been recently introduced predicts the arising of innovative computational solutions in the following years for an analytical field that increases data complexity. The IM-MS analysis shall rely in effective software that assists in the processes of data pretreatment and data analysis.

### 3 | DATA PRE-TREATMENT

As reviewed in the previous section, IM produces large sets of data that can be, at the same time, of different types depending on the acquisition modes used. Some of this data must be treated and prepared before it can be further analyzed and investigated. Particularly, we refer here to the demultiplexing of multiplexed files and other preprocessing steps, and to the subsequent CCS calculation. Different proprietary software has been developed by the vendors, which is exclusive for their users. For that reason, we will focus here and in the next section on free software offered by research groups and organizations.

#### 3.1 | Demultiplexing and other pre-processing tools

Multiplexing provides several advantages in terms of improved signal-to-noise and detector saturation. However, to visualize these benefits, multiplexed data files must be demultiplexed. This can be made via a proprietary software or a new and accessible software like the PNNL PreProcessor [30], developed by the Pacific Northwest National Laboratory. This uses an improved Hadamard-transform to perform demultiplexing and reconstruct data which also removes data artifacts [33]. Besides, PNNL PreProcessor is not just a demultiplexing tool, but it provides different modules for other preprocessing steps including the IM dimension, like smoothing, noise reduction, and saturation repair, among others. All of this is aimed at file simplification, user convenience and time saving as data complexity has drastically increased with IM [31, 32]. The preprocessing options that it includes can be used for DTIMS and SLIM analyses, in either scan or fragmentation data, and the preprocessing output files can be used for further analyses like feature finding and CCS calculation. The use of some of its features have been proven to be very practical in LC-IM-MS lipidomics by increasing the number of annotated lipids and decreasing processing time. For example, an increase of 19.4% in the number of lipid annotations was found when applying smoothing, noise reduction and saturation repair, furthermore, processing time was reduced by half [30]. In a different study, the number of detected features in human plasma, serum and HepG2 cells was about 20% more than in raw data when applying PNNL Preprocessor's smoothing, and noise filtering [64]. These results highlight the importance of a good and efficient data preprocessing

step in lipid annotation, especially when a complex third dimension is added to the analysis. PNNL Pre-Processor has also been used in other lipidomic studies within the last 2 years for demultiplexing and saturation repair [65–70], which shows a good acceptance of the software for these studies using IM-MS.

### 3.2 | CCS calculation

The CCS is a unique physical property determined by the size and shape of a molecule and the chemical and physical nature of the interaction with another molecule [71]. The CCS is defined as an “effective area” that quantifies the likelihood of a scattering event occurring when two species collide, in this case, the molecule analyzed and the buffer gas molecule, under the influence of an electric field. It is typically denoted as  $\sigma$  or  $\Omega$  and measured in units of area. Ions with a larger CCS are going to present more interaction with the gas, meaning that they will travel slower than those with smaller CCS values. Furthermore, the electric force experienced by an ion is proportional to their charge state, hence, ions with higher charge state will travel at a higher velocity. The arrival time, along with the specific conditions, can be directly translated into the CCS of the molecule using the Mason-Schamp equation [13, 19]:

$$\Omega = \frac{3ze}{16NK_0} \sqrt{\frac{2\pi}{\mu k_B T}}; K_0 = \frac{L}{t_A E} \frac{P}{P_0} \frac{T_0}{T}$$

where  $\Omega$  is the rotationally averaged CCS,  $k_B$  the Boltzman constant,  $T$  the temperature of the buffer gas,  $\mu$  reduced mass of the analyte ion and the buffer gas,  $t_A$  the corrected arrival time,  $ze$  the charge state of the analyte ion,  $E$  the electric field,  $L$  the length of the drift cell,  $P$  the pressure in drift cell,  $N$  the number density in the drift cell,  $K_0$  the reduced mobility, and  $P_0$  y  $T_0$  the pressure and temperature in standard conditions, respectively.

One of the advantages of CCS values is their high reproducibility across different laboratories and instruments, making it a great measurement for lipid annotation [72]. The introduction of CCS to MS analyses helps in the task of reducing the number of misidentifications and increasing the confidence level of the different annotations using  $m/z$ , ideally distinguishing between different isomers. It is important to note that CCS and  $m/z$  are related so they are not completely orthogonal, providing the composite CCS- $m/z$  data a lower confidence level than the  $m/z$ -MS/MS [43]. This can be observed in lipids with increasing masses, such as fatty acids, lyso forms of phospholipids and triglycerides, which have also increased CCS values.

CCS values can be calculated in DTIMS, TWIMS, TIMS. However, few facts must be considered for this calculation. First, the use of a trap cell before the IM, besides increasing the duty cycle, allows pulsing ion packets separated by a few milliseconds in a way that an arrival time ( $t_A$ ) can be assigned to each of the ions reaching to the detector, obtaining an arrival time distribution. This arrival time is the time for each ion to reach the detector and includes the time spent

in trespassing sectors of the IM-MS that are not only the IM stage ( $t_0$ ), such as quadrupoles, collision cells or the TOF stage [18]. The arrival time must be subsequently corrected to assign each ion to the corresponding time spent in traversing only the electric field of the IM, what is called in DTIMS as drift time ( $t_d$ ):

$$t_A = t_d + t_0$$

Second, all parameters involved in the CCS calculation must be accurately known. In DTIMS, for example, these parameters are drift time, gas temperature, gas pressure in the drift cell, voltages, tube length... Although the tube length is constant and very similar among different produced units and the voltage is accurately controlled with precision electronics, slight variations can be observed in the gas pressure and the gas temperature. This is particularly important in long sequences of analyses in which the room temperature can significantly vary affecting the gas temperature. Third and last, in TWIMS the field is dynamic and nonuniform, and this affects the CCS calculation of ions. Moreover, the ion heating experienced at higher fields also affects the accuracy of the CCS value in TWIMS [73]. To overcome these limitations, a CCS calibration with ions of known CCS values is performed by infusion of a calibrant mix in the IM-MS system for correction. Two CCS calculation methods are distinguished here:

- Primary methods: Based on experiments with several field values and called “stepped-field” calibrations for that reason, these calibrations are based on plotting the different  $t_A$  obtained versus the inverse drift voltages, only in DTIMS. A linear regression is calculated, from which  $t_0$  is calculated from the intercept and  $K_0$  (the reduced mobility used for interlaboratory comparisons) is proportional to the slope [74]. At least six different fields are used for this purpose [18]. These calibrations provide very accurate and reproducible CCS values with very high precision in interlaboratory comparisons. This was evaluated by Stow et al. 2017 [19] in three different laboratories, providing RSD values of 0.29% for several types of molecular classes in DTIMS. However, CCS values must be calculated one by one for the compounds of interest, which typically limits its use to the definition of CCS values for new compounds.
- Secondary methods: These methods can be done in DTIMS, TWIMS and TIMS and use a linear regression, reference compounds of known CCS values and a single field measure. For that reason, it is more practical and has been more widely accepted for CCS calculation [74, 75]. However, it provides less accurate CCS values having been shown to provide RSD values of 0.54% in DTIMS in the interlaboratory evaluation afore mentioned [19], while in TWIMS the deviations are higher for the reasons explained below. Still, these methods are found for most of the IM-MS applications, for comparisons and for CCS-assisted annotation.

The CCS should be reported as stated by McLean and Gabelica, including the drift gas and the instrument type in the terminology such as  $^{DT}CCS_{N_2}$  (for values obtained in DTIMS using  $N_2$  as drift gas) or  $^{TW}CCS_{N_2}$  (for values obtained in TWIMS using  $N_2$  as drift gas), as



well as including whether they were determined using a primary or secondary method [74, 76]. This is relevant since the CCS calibration entails important differences among DTIMS, TWIMS, TIMS. For example, DTIMS shows lower RSD in the determination of CCS than TWIMS. Moreover, TWIMS requires the use of compounds with similar structures to the ones whose CCS wants to be calculated. This poses an important problem, considering that a wide variety of compounds can be found in a single sample. This was evaluated by Hines and collaborators [77], whose work evaluated the use of different CCS calibrants for the determination of the CCS in lipids, from the generic poly-Ala used in TWIMS to more specific phospholipids. The authors observed higher accuracies when phospholipids were used as calibrants, which has higher similarity to the analytes than poly-Ala, which gave less accurate CCS values. Moreover, the authors observed better calibrations in positive ionization mode using phosphatidylcholines and in negative ionization mode using phosphatidylethanolamines. Although this greatly overcomes the problem of the accuracy in the CCS values obtained in TWIMS, entangles a problem of correctly choosing the calibrant in TWIMS. A recent approach allows the CCS calculation in DMS using a machine learning-based calibration [78]. However, these are not experimentally calculated CCS values, but based on predictive models, providing CCS within 2.6% mean absolute percentage error. In this case, the type of molecules used for the training set of the predictive model also affect in a great extent the calculated CCS and different models should be used for different analytes. This makes this approach, although feasible, far from being a routine process for the CCS calculation. Summarizing, the type of IM used and the experimental conditions during the calibration greatly affect the accuracy of the estimated CCS value. For more detailed information about CCS calibrations in different IM systems, refer to more specific literature on the topic [3, 72–74, 77, 79].

In a routine IM-MS analysis CCS values are not determined manually, but they are usually determined using proprietary software provided by the vendors such as IM-MS Browser from Agilent and Progenesis Q1 from Waters, which somehow can limit the accessibility and possibilities of analysis. Different freely available software has been developed to make CCS calculations more convenient and open like PIXiE [80] and AutoCCS [75] which are further discussed below.

PIXiE is an open-source tool for CCS calculation based on primary methods. The fact that secondary methods are not supported was justified by the desired accuracy of the reported CCS values by PIXiE [80]. Their creators further developed PIXiE into what was later called AutoCCS. This upgraded version can perform CCS calculations for Agilent (DTIMS) 6560, stepped-field and single-field methods, as well as for Waters SynaptG2s-i (TWIMS) and for Bruker timTOF Pro™ (TIMS). It is worth noting that for DTIMS single-field calibration, two methods are available, one of them offering more accurate CCS values, since it accounts for temperature and pressure variations that typically occur during the analysis to correct them. Its performance was tested on Agilent's tune-mix ions for all the calibration methods and for some metabolites and peptides in stepped-field and single-field methods in DTIMS. The obtained CCS values with AutoCCS were compared to 3 reference sets of CCS values, being the error (%) always below 1%.

Data including the list of IM-MS features can be uploaded as MZmine and csv files, among other proprietary formats. The main advantage of AutoCCS, apart from the fact of accepting open-source format files for data input and being usable with IM-MS data from any instrument, is the time saving during the generation of the CCS values through an automated workflow [75].

## 4 | DATA ANALYSIS

### 4.1 | IM-MS computational resources for metabolite identification

The CCS values obtained and calculated by IM means have been included in the process of metabolite annotation since it provides a quasi-orthogonal property of the analyzed molecules. Furthermore, the high reproducibility of the CCS among different laboratories [19] makes its use trivial to use as a filter since this property might be used to perform metabolite annotation and reduce the false positive annotation rate [3, 66, 79]. An effort to outline the standards to report the IM-MS measurements was done by Gabelica et al. [74] with the goal of exploiting the CCS values obtained in different experiments, and a number of metabolomic databases have reported or included the CCS values of their compounds. As the CCS value will vary depending on the adduct formed, the databases should provide them for the most common ones.

### 4.2 | CCS experimental databases

Table 1 summarizes the current metabolomic databases providing experimental CCS values that are accessible through a programmatic way or in an easily readable format. This aspect is relevant for the use of the CCS libraries to create models able to predict the CCS of compounds yet to experimentally analyze, since the experimental analysis of all the metabolomes is unfeasible. CCS Compendium [52] is a unified compendium of about 3800 experimentally CCS values; the IM conformational lipid atlas for high confidence lipidomics [1], accessible from LipidMaps; the IM collision cross-section atlas, known as AllCCS by its web interface was released in 2020 and published about 5000 CCS values [67]; the database from CCSBase created in order to train a model for predicting CCS values [81]; and finally the one recently announced by XCMS from the Gary Siuzdak group of Scripps, which contains above 10,000 reference compounds with their corresponding experimental CCS values and its accessible under a payment license through the XCMS Online [82].

### 4.3 | CCS predicted databases and predictive tools

The databases containing experimental data are always preferred by the researchers, but the lack of experimental CCS values makes the prediction of them a must to annotate metabolites in experiments

**TABLE 1** Characteristics of metabolomic databases with experimental CCS values

	CCS compendium	CCS base	Pacific northwest national laboratory	LipidMaps	AllCCS
Size of data set	3,728 values (1,714 compounds)	12,577 values (5,077 compounds)	>500 values	456 values (217 compounds)	3359 values (2193 compounds)
Number of adducts	18 <sup>a</sup>	45 <sup>b</sup>	9 <sup>c</sup>	7 <sup>c</sup>	15 <sup>d</sup>
Diversity of compounds	14 superclasses, 80 classes and 157 subclasses	Small molecules, lipids, peptides and carbohydrates	Primary and secondary metabolites and xenobiotics	7 lipid classes	14 classes, 144 classes and 257 subclasses
Measurement technique	DTIM and TWIM	DTIM and TWIM	DTIM	DTIM	DTIM and TWIM
Buffer gas	Nitrogen	Nitrogen	Nitrogen	Nitrogen	Nitrogen
Format	CSV file	CSV, SQL dump and web interface	TSV	XSLX, web interface and Rest API	Web interface
Downloadable	✓	✓	✓	✓	✗
Compendium	✓	✓	✗	✗	✓
Contained in other compendiums	✗	✗	✓	✓	✗
Access	Free	Free	Free	Free	Free, requires registration

<sup>a</sup>Adducts: [M-2H]<sup>2-</sup>, [M-2H+Na]<sup>+</sup>, [M-Br+O]<sup>-</sup>, [M-Cl+O]<sup>-</sup>, [M-H-H<sub>2</sub>O]<sup>-</sup>, [M-H]<sup>-</sup>, [M-H+H<sub>2</sub>O]<sup>-</sup>, [M]<sup>+</sup>, [M+2H]<sup>2+</sup>, [M+2H+K]<sup>3+</sup>, [M+3H]<sup>3+</sup>, [M+4H]<sup>4+</sup>, [M+5H]<sup>5+</sup>, [M+Cu]<sup>2+</sup>, [M+H-H<sub>2</sub>O]<sup>+</sup>, [M+H]<sup>+</sup>, and [M+Na]<sup>+</sup>.

<sup>b</sup>Adducts: [M-2H]<sup>2-</sup>, [M-2SO<sub>3</sub>-2H<sub>2</sub>O+H]<sup>+</sup>, [M-CH<sub>3</sub>]<sup>-</sup>, [M-H]<sup>-</sup>, [M-H<sub>2</sub>O-H]<sup>-</sup>, [M-H<sub>2</sub>O+H]<sup>+</sup>, [M-H<sub>2</sub>O+HCOO]<sup>-</sup>, [M-SO<sub>3</sub>-3H<sub>2</sub>O+H]<sup>+</sup>, [M-SO<sub>3</sub>-H]<sup>-</sup>, [M-SO<sub>3</sub>-H<sub>2</sub>O-H]<sup>-</sup>, [M-SO<sub>3</sub>-H<sub>2</sub>O+Cl]<sup>-</sup>, [M-SO<sub>3</sub>-H<sub>2</sub>O+H]<sup>+</sup>, [M-SO<sub>3</sub><sup>2-</sup>-H<sub>2</sub>O+HCOO]<sup>-</sup>, [M-SO<sub>3</sub>+Cl]<sup>-</sup>, [M]<sup>+</sup>, [M+2H]<sup>2+</sup>, [M+2K]<sup>2+</sup>, [M+2Na-3H]<sup>-</sup>, [M+2Na-H]<sup>+</sup>, [M+3H]<sup>3+</sup>, [M+4H]<sup>4+</sup>, [M+CH<sub>3</sub>COO]<sup>-</sup>, [M+Cl]<sup>-</sup>, [M+Cs]<sup>+</sup>, [M+H-2H<sub>2</sub>O]<sup>+</sup>, [M+H-H<sub>2</sub>O]<sup>+</sup>, [M+H]<sup>+</sup>, [M+H<sub>2</sub>O-H]<sup>-</sup>, [M+H<sub>3</sub>C<sub>2</sub>O<sub>2</sub>]<sup>-</sup>, [M+HCOO]<sup>-</sup>, [M+K-2H]<sup>-</sup>, [M+K-H+Cl]<sup>-</sup>, [M+K-H+HCOO]<sup>-</sup>, [M+K]<sup>+</sup>, [M+Li]<sup>+</sup>, [M+Na-2H]<sup>-</sup>, [M+Na-2H<sub>2</sub>O]<sup>+</sup>, [M+Na-H]<sup>+</sup>, [M+Na-H+Cl]<sup>-</sup>, [M+Na-H+HCOO]<sup>-</sup>, [M+Na-H<sub>2</sub>O]<sup>+</sup>, [M+Na]<sup>+</sup>, [M+NH<sub>4</sub>]<sup>+</sup>, [M+OAcO]<sup>-</sup>, and [M+Rb]<sup>+</sup>.

<sup>c</sup>Adducts: [M+H]<sup>+</sup>, [M+Na]<sup>+</sup>, [M-H]<sup>-</sup>, [M+2H]<sup>2+</sup>, [M]<sup>+</sup>, [M+CH<sub>3</sub>COO]<sup>-</sup>, [M+HCOO]<sup>-</sup>, [M-Br+O]<sup>-</sup>, and [M-Cl+O]<sup>-</sup>.

<sup>d</sup>Adducts: [M+Na]<sup>+</sup>, [M+2Na-H]<sup>+</sup>, [M+H]<sup>+</sup>, [M+K]<sup>+</sup>, [M-H]<sup>-</sup>, [M+Cl]<sup>-</sup>, [M+HCOO]<sup>-</sup>, [M+Na-H<sub>2</sub>O]<sup>+</sup>, [M+H-2H<sub>2</sub>O]<sup>+</sup>, [M+H-H<sub>2</sub>O]<sup>+</sup>, and [M+Na-2H<sub>2</sub>O]<sup>+</sup>.

using IM as a separation technique. Thus, a considerable number of alternatives to predict them has been developed. Historically, it has been several methods that calculate the CCS using different theoretical models, such as MOBCAL [83], Sigma Suite [84], WebPSA [85], IMPACT [86], CCS [87], Collidoscope [88], ISICLE [89], or HPCCS [90]. Most of them have a better performance the larger the molecule is and, therefore, they are mostly used in the proteomics field.

Recently, with the publication of several experimental data sets previously mentioned, different machine learning models have arisen. MetCCS [91], LipidCCS [92], DeepCCS [93], CCSBase [94], AllCCS [67], or DarkChem [95] are some of the examples, all showing median relative errors below 3% in the calculation of CCS. Some of them provide a web interface that ease the use of researchers with a small background in computer programming. The high precision of these solutions helps to overcome the lack of experimental databases, which are slowly being published. The characteristics of these predictive tools are presented in

Table 2, excluding the alternatives whose source code or any interface to use them were unavailable [96–99]. Furthermore, some of the most used databases to annotate metabolites such as HMDB [100] or Metlin [82] (under payment) have incorporated CCS values to filter the annotations based on the *m/z* and the CCS values, and optionally to perform similarity spectra searches.

#### 4.4 | CCS identification software tools

Regardless the high precision of the IM instrumentation, the growing number of CCS databases for known structures and the improvement in the computational tools to predict the CCS, it does not seem that the experimentally collected data will be enough during the next few years to distinguish a unique structure among isomers with a highly similar structure. This is especially noticeable in those cases where the sample only contains one of them and it is

**TABLE 2** Characteristics of CCS predictive tools

	CCSBase	DeepCCS	DarkChem	AIICCS	LipidCCS	IsiCICLE <sup>a</sup>	MetCCS
Size of CCS data set to train the model	7,405 values	1,260 values	~2,400 values	3,539 values	458 values	Uses a quantum chemistry pipeline, not a ML model	Not stated
API availability							
API Programming language	N/A	Python	Python	N/A	N/A	Python	N/A
Prior requirements	None	Numpy, Pandas, Scikit-learn, Tensorflow and Keras	Numpy, Pandas, Scikit-learn, Tensorflow, Keras, scipy, Rdkit and OpenBabel	Registration			
None							
Not tested	Calculation of molecular descriptors of the molecule						
Number of adducts	8 <sup>b</sup>	4 <sup>c</sup>	3 <sup>d</sup>	7 <sup>e</sup>	5 <sup>f</sup>	Not tested	5 <sup>g</sup>
Entry format	CSV or single SMILES	CSV	CSV	CSV, manual or SMILES	CSV, TXT or single SMILES	Not tested	CSV, TXT or molecular features
Output Format	CSV or online view	CSV or command line	TSV	CSV or online view	CSV or Online view	Not tested	Online view
Maximum predictions per execution	~2,000	Unlimited	Unlimited	50	50	Not tested	10
Last update	August 2021	April 2019	March 2021	October 2021	Jun 2017	April 2020	March 2017
User-Friendly <sup>h</sup>						Not tested	
Descriptive Error Capacity in local execution					N/A	N/A	N/A

<sup>a</sup> IsiCICLE was not tested as it requires a ChemAxon payment license to be executed.

<sup>b</sup> [M+H]<sup>+</sup>, [M+Na]<sup>+</sup>, [M+NH<sub>4</sub>]<sup>+</sup>, [M+K]<sup>+</sup>, [M+H]<sup>-</sup>, [M+Na-2H]<sup>-</sup>, [M]<sup>+</sup> and [M]<sup>-</sup>

<sup>c</sup> [M+H]<sup>+</sup>, [M+Na]<sup>+</sup>, [M+H]<sup>-</sup> and [M-2H]<sup>2-</sup>

<sup>d</sup> [M+H]<sup>+</sup>, [M+H]<sup>-</sup> and [M+Na]<sup>+</sup>

<sup>e</sup> [M+H]<sup>+</sup>, [M+H-H<sub>2</sub>O]<sup>+</sup>, [M+Na]<sup>+</sup>, [M+NH<sub>4</sub>]<sup>+</sup>, [M+H]<sup>-</sup>, [M+Na-2H]<sup>-</sup>, and [M+HCOO]<sup>-</sup>

<sup>f</sup> [M+H]<sup>+</sup>, [M+Na]<sup>+</sup>, [M+NH<sub>4</sub>]<sup>+</sup>, [M+H]<sup>-</sup> and [M+HCOO]<sup>-</sup>

<sup>g</sup> [M+H]<sup>+</sup>, [M+H-H<sub>2</sub>O]<sup>+</sup>, [M+Na]<sup>+</sup>, [M+H]<sup>-</sup> and [M+Na-2H]<sup>-</sup>

<sup>h</sup> User-friendly is a subjective appreciation by the authors based on how easy and intuitive the tools were, the available documentation, and the descriptive capacity of the errors produced by each tool.

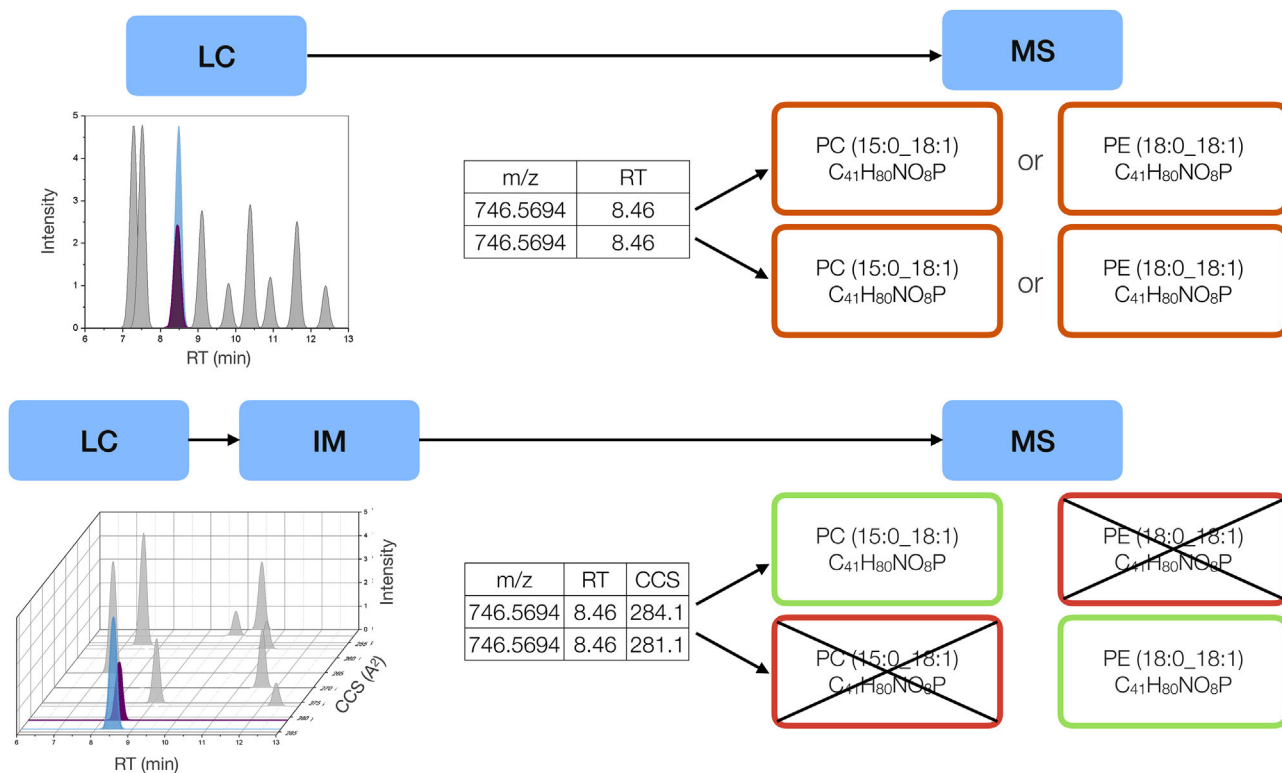


**FIGURE 6** The inclusion of a quasi-orthogonal dimension like CCS provides evidence to support or refute an annotation, resulting in the increasing of the precision and the recall of the annotated metabolites, especially for novel researchers that do not have the expertise to interpret RT information.

necessary to elucidate the right identification. The CCS similarity might provide evidence to support or to refute one or several structures from the others, but the precision of the current instrumentation is not sufficient to uniquely identify one. Figure 6 shows an example of how two lipids could be differentiated using their CCS values. The low reproducibility of RT hampers its interpretation, but the high reproducibility of CCS makes the difference ( $\Delta$ CCS) between the experimental CCS and the reference ones (contained in databases or predicted by computational tools) ideal for novel researchers that might not have enough experience to use the RT to identify the analyzed features, but they can easily interpret the  $\Delta$ CCS. Thus, the CCS similarity increases the confidence in the annotation of putative candidates of features, although the high correlation between the CCS and the  $m/z$  values [14, 48, 53, 101] hinders the unique identification of metabolites using the information coming from LC-IM-MS experiments. The CCS value together with the  $m/z$  is not sufficient to uniquely identify features, especially in biological samples with a large number of metabolites present without prior knowledge, but it provides hints about which one is more plausible. Thus, the configuration LC-IM-MS/MS has become the most common setup when incorporating IM to the metabolomics and lipidomics workflows resulting in the improvement of the MS/MS spectra quality and easing the identification using all the orthogonal information available ( $m/z$ , RT, CCS and MS/MS fragments). This comes at the cost of analyzing a larger amount

of information from each feature, but the effort has been demonstrated worthy.

There is an extensive literature bibliography where the use of IM permits the profiling and the quantification of isomers and isobars [3, 102], but the expert knowledge from the researchers has been applied to create a methodology that permits to analyze the experiments to reach that. Particularly, correlations between the dimensions of a 2D separation create trend lines that depend on structural or chemical characteristics of the compound class and thus facilitate classification of unknowns. This broadly applies to conventional IM-MS, where the major biomolecular classes (e.g., lipids, peptides, nucleotides) occupy different trend line domains [4, 18, 48, 53, 103]. Lipids occupy different spaces, showing some lipid classes a larger CCS respecting some other ones [3, 79]. The degree of unsaturation of fatty acyl chains also affects the CCS, reducing the drift time about 1%–5% for each double bond [104].

A promising alternative to analyze information coming from different orthogonal properties in this configuration ( $m/z$ , RT, CCS and MS/MS fragments) is the creation of expert systems that provide evidence to support or refute the annotations [13]. Computational tools like MS-Dial [105], SIFTER [106], Lipid4DAnalyzer [66], Skyline [107] or CEU Mass Mediator [108] are a promising approach to incorporate the CCS information to its knowledge base in addition to other dimensions such as the Kendrick Mass Defect, the RT and/or

**TABLE 3** Summary of the publications in which CCS values were used for lipid identification

Analyzer	Lipid identification	Lipid Class(es)	Confidence Level by MSI	Biological Sample	Cite
Synapt G2 HDMS, Waters	Experimental		Level 2	Brain tissue	[3]
Agilent 6560 Drift Tube-Ion Mobility-Q-ToF	Experimental and predicted	DG, PC, TG, LPE, SM	Level 3	Bovine milk	[4]
Waters Synapt G2-Si HDM	Experimental	MG, DG, DGDG, CL, PA, lysyl-PG	Level 2	<i>Enterococcus faecalis</i> , <i>Staphylococcus aureus</i> and <i>Corynebacterium striatum</i>	[6]
Agilent 6560 Drift Tube-Ion Mobility-Q-ToF	Experimental	Oxylipins	Level 2	Mouse lung tissue	[10]
Agilent 6560 Drift Tube-Ion Mobility-Q-ToF	Predicted	DG, PC, TG, LPE, SM	Level 3	Human plasma samples, NIH 3T3 samples (a mouse embryo fibroblast cell line), and mouse brain tissue samples	[31]
Agilent 6560 Drift Tube-Ion Mobility-Q-ToF	Experimental and predicted		Level 2 and 3	HepaRG cells	[37]
Agilent 6560 Drift Tube-Ion Mobility-Q-ToF	Experimental	Oxylipins	Level 2	Plasma, serum and cells	[45]
Agilent 6560 Drift Tube-Ion Mobility-Q-ToF	Experimental	Oxylipins	Level 2	<i>Salmonella typhimurium</i> - infected murine bone marrow derived macrophages (BMDM) and thrombin activated human platelets	[46]
Agilent 6560 Drift Tube-Ion Mobility-Q-ToF	Experimental		Level 3	Human plasma and bronchoalveolar lavage fluid (BALF)	[48]
Agilent 6560 Drift Tube-Ion Mobility-Q-ToF	Experimental		Level 2	Rat brain tissue	[49]
Agilent 6560 Drift Tube-Ion Mobility-Q-ToF	Experimental		Level 2	Human serum	[52]
Synapt G2-S instrument	Experimental	PC, PE, PI, PA, PS, SM	Level 2 and 3	Human serum	[54]
timsTOFflex Bruker	Experimental		Level 3	Mouse spleen tissue	[61]
Agilent 6560 Drift Tube-Ion Mobility-Q-ToF	Predicted		Level 3	Human plasma, human serum and HepG2 cells	[64]
Agilent 6560 Drift Tube-Ion Mobility-Q-ToF	Experimental	Sterols	Level 2	Mouse brain tissue	[65]
Agilent 6560 Drift Tube-Ion Mobility-Q-ToF	Experimental	GP, SP, GL, FA and 25 lipid classes	Level 2	Human plasma, 293T cells, mouse liver and brain tissues	[66]
Waters Synapt G2-Si HDMS	Experimental		Level 2	Neuroblastoma	[79]
Waters Synapt G2-Si HDMS	Experimental and predicted		Level 3	Methicillin-resistant <i>Staphylococcus aureus</i> (MRSA)	[81]
Agilent 6560 Drift Tube-Ion Mobility-Q-ToF	Experimental	PC	Level 2	Human cell pellets, mouse tissue and human plasma	[92]

the fragmentation spectra to improve the metabolite annotation and identification in metabolomics.

- MS-DIAL 4 [105] shows that the inclusion of the CCS information (together with RT,  $m/z$ , isotropic ions, adduct information and MS/MS fragmentations) increases confidence annotating and semi-quantifying 8051 lipids with a 1%–2% estimated false discovery rate. CCS information combined with the new acquisition and data processing approaches enables 8051 lipids from 117 lipid subclasses to be identified between Level 1 (identified by standard compound) and Level 3.2 (accurate mass spectrum and number of carbons confirmed).
- Skyline [48, 107] was updated to support IM-MS data to permit an automated data analysis of the huge datasets generated by these systems. Skyline supports scan and MS/MS data, including DIA and DDA and some specific acquisition modes, such as DIA-PASEF or DIA-SWATH. The proposed workflow by Skyline focuses on targeted or semitargeted metabolomics. The lipidomic annotation workflow consists in the creation of a personal library created by the user (semitargeted), or the human plasma lipid library published by its team consisting of 516 unique lipids. Libraries can include MS/MS spectra, name, formula, adduct,  $m/z$ , RT and CCS values. Skyline offers data visualization to inspect chromatograms and spectra by filtering by the DT which permits an intuitive data visualization due to the IM filtering of noise, isomers and isobars.
- Lipid4DAnalyzer, previously known as LipidIMMS [66], is an expert system processing multidimensional information from the mass spectrometer ( $m/z$ ), the separation techniques (RT, CCS) and the fragmentation spectra (MS/MS) for lipid identification. The tool covers 4 superclasses, 25 classes and 267,716 *in silico* lipid structures. For each lipid the CCS values were predicted using LipidCCS; RTs were predicted using a Random Forest (RF) algorithm; and MS/MS spectra were predicted using fragmentation rules. Then, it compares the experimental data with the generated one using a parametrizable rule-based approach that permits ranking the candidates for identification.
- SIFTER [106] presented a machine learning algorithm to identify compounds based on the  $m/z$ , the CCS and the Kendrick Mass Defect instead of another separation technique. The main novelty of this approach is the usage of the Kendrick Mass Defect to predict the chemical class, thus providing evidence to support the identification of functional group isomers. It claims a right category classification around 80%.

There are several publications that have already used the IM techniques and the CCS property to perform metabolite identification. Table 3 summarizes those publications according to the instrumentation used, the metabolite identification confidence level, the metabolites type, and the tissue where the metabolites were identified is shown.

The growing number of experimentally collected CCS databases and libraries will aid the development of improved models to predict the CCS of molecules, as well as they will help to create the expert sys-

tems to incorporate knowledge regarding a new orthogonal property, but the high similarity between some isomers hampers the direct use of the CCS to distinguish them. This limitation does not reduce the potential of the inclusion of IM in metabolomic experiments. LC-IM-MS/MS experiments (1) permit the separation of otherwise coeluting compounds, thus permitting the proper analysis of the separated features and the acquisition of a higher quality MS/MS spectra; (2) provide a reproducible orthogonal property to properly identify among isomers with a considerable different shape and size structure; (3) provide evidence to support or refute the candidate structures; and (4) thus results in providing a higher confidence level with (confidence level 1) or without the use of reference standards (confidence level 3). The community as a whole should work in facilitating the communication between the different tools providing APIs and free access to the tools. As the IM-MS field is still in an early stage, we shall focus on the open-science, providing all source codes, documentation and data, so other researchers can contribute to the field.

## 5 | CONCLUSIONS

When coupled to MS instrumentation, IM has shown to be a great tool to enhance the confidence level in metabolite identification, especially in lipidomics studies. Continuous improvements in data acquisition approaches, mainly in the direction of a higher resolution and a higher quality spectrum, are enabling a more comprehensive lipidome coverage. New DDA and DIA MS/MS such as PASEF, TAP of QRAI and other fragmentation methodologies provide novel tools for better lipid characterization. In combination with new hardware like SLIM and cyclic TWIMS for HRIM and the multiple possibilities of front-end separation techniques permit the in-depth analysis and elucidation of lipids and their isomers. IM-MS is evolving fast and the emergence of new instrumental designs, acquisitions modes and software tools for data treatment, analysis and feature identification are continuously being developed. The combination of different approaches multiplies the generated data in a way that studying it manually in detail becomes an unfeasible task in most lipidomics studies. For that reason, new developments in software and data treatment have come to help the researchers analyzing and interpreting their data. The high reproducibility of the CCS across different laboratories and instruments and the increasing experimental databases, with the more refined *in silico* prediction tools and annotation software tools such as Lipid4DAnalyzer, MS-DIAL 4 or SIFTER considerably aid in the identification of lipids. Moreover, software tools that help automatize data analysis are making this technique more accessible to researchers not just in academia, but in industry and clinical settings [109].

Most of these developments have appeared recently, therefore it is reasonably expected that innovative advances in IM-MS will expand during the next years. However, the number of open-source computational tools for the IM-MS data analysis is relatively low. Most of the data analysis in IM-MS experiments is performed using proprietary tools provided by the vendors. On the contrary, it seems that specific-task tools are slowly being released. Skyline might be an exception,

providing a complete software tool for the IM-MS/MS data analysis. The creation and adoption of a standard file format from the vendors seems a good solution to enhance the interoperability of tools. The analytical community shall work in the creation of standard routines to acquire and analyze the data obtained.

## ACKNOWLEDGMENT

Maria Moran-Garrido thanks her predoctoral fellowship to the Ministry of Universities grant number FPU19/06206. Sandra M. Camunas-Alberca thanks her contract associated to the project funded by Fundación La Caixa Grant HR17-00634.

## CONFLICT OF INTEREST

The authors declare no conflict of interest.

## DATA AVAILABILITY STATEMENT

No data was used in the preparation of this review that can be available for the readers.

## ORCID

Coral Barbas  <https://orcid.org/0000-0003-4722-491X>

## REFERENCES

1. Leaprot, K. L., May, J. C., Dodds, J. N., & Mclean, J. A. (2019). Ion mobility conformational lipid atlas for high confidence lipidomics. *Nature Communications*, 10, 985.
2. Köfeler, H. C., Ahrends, R., Baker, E. S., Ekroos, K., Han, X., Hoffmann, N., Holčapek, M., Wenk, M. R., & Liebisch, G. (2021). Recommendations for good practice in MS-based lipidomics. *Journal of Lipid Research*, 62, 100138.
3. Paglia, G., Angel, P., Williams, J. P., Richardson, K., Olivos, H. J., Thompson, J. W., Menikarachchi, L., Lai, S., Walsh, C., Moseley, A., Plumb, R. S., Grant, D. F., Palsson, B. O., Langridge, J., Geromanos, S., & Astarita, G. (2015). Ion mobility-derived collision cross section as an additional measure for lipid fingerprinting and identification. *Analytical Chemistry*, 87, 1137–1144.
4. Blaženović, I., Shen, T., Mehta, S. S., Kind, T., Ji, J., Piparo, M., Cacciola, F., Mondello, L., & Fiehn, O. (2018). Increasing compound identification rates in untargeted lipidomics research with liquid chromatography drift time–ion mobility mass spectrometry. *Analytical Chemistry*, 90, 10758–10764.
5. Monge, M. E., Dodds, J. N., Baker, E. S., Edison, A. S., & Fernández, F. M. (2019). Challenges in identifying the dark molecules of life. *Annual Review of Analytical Chemistry*, 12, 177–199.
6. Hines, K. M., Waalkes, A., Penewit, K., Holmes, E. A., Salipante, S. J., Werth, B. J., & Xu, L. (2017). Characterization of the mechanisms of daptomycin resistance among gram-positive bacterial pathogens by multidimensional lipidomics. *mSphere*, 2, e00492–17.
7. Ahonen, L., Fasciotti, M., Gennäs, G. B. Af, Kotiaho, T., Daroda, R. J., Eberlin, M., & Kostianen, R. (2013). Separation of steroid isomers by ion mobility mass spectrometry. *Journal of Chromatography A*, 1310, 133–137.
8. Groessl, M., Graf, S., & Knochenmuss, R. (2015). High resolution ion mobility-mass spectrometry for separation and identification of isomeric lipids. *Analyst*, 140, 6904–6911.
9. Bowman, A. P., Abzalimov, R. R., & Shvartsburg, A. A. (2017). Broad separation of isomeric lipids by high-resolution differential ion mobility spectrometry with tandem mass spectrometry. *Journal of The American Society for Mass Spectrometry*, 28, 1552–1561.
10. Kyle, J. E., Aly, N., Zheng, X., Burnum-Johnson, K. E., Smith, R. D., & Baker, E. S. (2018). Evaluating lipid mediator structural complexity using ion mobility spectrometry combined with mass spectrometry. *Bioanalysis*, 10, 279–289.
11. May, J. C., & McLean, J. A. (2015). Ion mobility-mass spectrometry: Time-dispersive instrumentation. *Analytical Chemistry*, 87, 1422–1436.
12. Gabelica, V., & Marklund, E. (2018). Fundamentals of ion mobility spectrometry. *Current Opinion in Chemical Biology*, 42, 51–59.
13. Dodds, J. N., & Baker, E. S. (2019). Ion mobility spectrometry: Fundamental concepts, instrumentation, applications, and the road ahead. *Journal of The American Society for Mass Spectrometry*, 30, 2185–2195.
14. D'atri, V., Causon, T., Hernandez-Alba, O., Mutabazi, A., Veuthey, J.-L., Cianferani, S., & Guilleme, D. (2018). Adding a new separation dimension to MS and LC-MS: What is the utility of ion mobility spectrometry? *Journal of Separation Science*, 41, 20–67.
15. Cumeras, R., Figueras, E., Davis, C. E., Baumbach, J. I., & Gràcia, I. (2015). Review on ion mobility spectrometry. Part 1: Current instrumentation. *Analyst*, 140, 1376–1390.
16. Richardson, K., Langridge, D., & Giles, K. (2018). Fundamentals of travelling wave ion mobility revisited: I. Smoothly moving waves. *International Journal of Mass Spectrometry*, 428, 71–80.
17. Shvartsburg, A. A., & Smith, R. D. (2008). Fundamentals of traveling wave ion mobility spectrometry. *Analytical Chemistry*, 80, 9689–9699.
18. May, J. C., Goodwin, C. R., Lareau, N. M., Leaprot, K. L., Morris, C. B., Kurulugama, R. T., Mordehai, A., Klein, C., Barry, W., Darland, E., Overney, G., Imatani, K., Stafford, G. C., Fjeldsted, J. C., & McLean, J. A. (2014). Conformational ordering of biomolecules in the gas phase: Nitrogen collision cross sections measured on a prototype high resolution drift tube ion mobility-mass spectrometer. *Analytical Chemistry*, 86, 2107–2116.
19. Stow, S. M., Causon, T. J., Zheng, X., Kurulugama, R. T., Mairinger, T., May, J. C., Rennie, E. E., Baker, E. S., Smith, R. D., McLean, J. A., Hann, S., & Fjeldsted, J. C. (2017). An interlaboratory evaluation of drift tube ion mobility-mass spectrometry collision cross section measurements. *Analytical Chemistry*, 89, 9048–9055.
20. Deng, L., Ibrahim, Y. M., Hamid, A. M., Garimella, S. V. B., Webb, I. K., Zheng, X., Prost, S. A., Sandoval, J. A., Norheim, R. V., Anderson, G. A., Tolmachev, A. V., Baker, E. S., & Smith, R. D. (2016). Ultra-high resolution ion mobility separations utilizing traveling waves in a 13 m serpentine path length structures for lossless ion manipulations module. *Analytical Chemistry*, 88, 8957–8964.
21. Giles, K., Ujma, J., Wildgoose, J., Pringle, S., Richardson, K., Langridge, D., & Green, M. (2019). A cyclic ion mobility-mass spectrometry system. *Analytical Chemistry*, 91, 8564–8573.
22. Michelmann, K., Silveira, J. A., Ridgeway, M. E., & Park, M. A. (2014). Fundamentals of trapped ion mobility spectrometry. *Journal of The American Society for Mass Spectrometry*, 26, 14–24.
23. Fouque, J. D., & K, F.-L. (2019). Recent advances in biological separations using trapped ion mobility spectrometry – mass spectrometry. *TrAC - Trends in Analytical Chemistry*, 116, 308–315.
24. Zhang, J. D., Mohibul Kabir, K. M., Lee, H. E., & Donald, W. A. (2018). Chiral recognition of amino acid enantiomers using high-definition differential ion mobility mass spectrometry. *International Journal of Mass Spectrometry*, 428, 1–7.
25. Wernisch, S., & Pennathur, S. (2019). Application of differential mobility-mass spectrometry for untargeted human plasma metabolomic analysis. *Analytical and Bioanalytical Chemistry*, 411, 6297–6308.
26. Baker, P. R. S., Armando, A. M., Campbell, J. L., Quehenberger, O., & Dennis, E. A. (2014). Three-dimensional enhanced lipidomics analysis combining UPLC, differential ion mobility spectrometry, and mass spectrometric separation strategies. *Journal of Lipid Research*, 55, 2432–2442.

27. Paglia, G., Smith, A. J., & Astarita, G. (2021). Ion mobility mass spectrometry in the omics era: Challenges and opportunities for metabolomics and lipidomics. *Mass Spectrometry Reviews*, 1–44.
28. Hines, K. M., & Xu, L. (2019). Lipidomic consequences of phospholipid synthesis defects in *Escherichia coli* revealed by HILIC-ion mobility-mass spectrometry. *Chemistry and Physics of Lipids*, 219, 15–22.
29. Dodds, J. N., May, J. C., & McLean, J. A. (2017). Correlating resolving power, resolution, and collision cross section: Unifying cross-platform assessment of separation efficiency in ion mobility spectrometry. *Analytical Chemistry*, 89, 12176–12184.
30. Bilbao, A., Gibbons, B. C., Stow, S. M., Kyle, J. E., Bloodsworth, K. J., Payne, S. H., Smith, R. D., Ibrahim, Y. M., Baker, E. S., & Fjeldsted, J. C. (2022). A preprocessing tool for enhanced ion mobility-mass spectrometry-based omics workflows. *Journal of Proteome Research*, 21, 798–807.
31. Zhou, Z., Shen, X., Chen, Xi., Tu, J., Xiong, X., & Zhu, Z.-J. (2019). LipidIMMS analyzer: Integrating multi-dimensional information to support lipid identification in ion mobility-mass spectrometry based lipidomics. *Bioinformatics*, 35, 698–700.
32. Maclean, B. X., Pratt, B. S., Egertson, J. D., Maccoss, M. J., Smith, R. D., & Baker, E. S. (2018). Using skyline to analyze data-containing liquid chromatography, ion mobility spectrometry, and mass spectrometry dimensions. *Journal of The American Society for Mass Spectrometry*, 29, 2182–2188.
33. Prost, S. A., Crowell, K. L., Baker, E. S., Ibrahim, Y. M., Clowers, B. H., Monroe, M. E., Anderson, G. A., Smith, R. D., & Payne, S. H. (2014). Detecting and removing data artifacts in hadamard transform ion mobility-mass spectrometry measurements. *Journal of The American Society for Mass Spectrometry*, 25, 2020–2027.
34. Causon, T. J., Si-Hung, Le., Newton, K., Kurulugama, R. T., Fjeldsted, J., & Hann, S. (2019). Fundamental study of ion trapping and multiplexing using drift tube-ion mobility time-of-flight mass spectrometry for non-targeted metabolomics. *Analytical and Bioanalytical Chemistry*, 411, 6265–6274.
35. Belov, M. E., Buschbach, M. A., Prior, D. C., Tang, K., & Smith, R. D. (2007). Multiplexed ion mobility spectrometry-orthogonal time-of-flight mass spectrometry. *Analytical Chemistry*, 79, 2451–2462.
36. Reinecke, T., Naylor, C. N., & Clowers, B. H. (2019). Ion multiplexing: Maximizing throughput and signal to noise ratio for ion mobility spectrometry. *TrAC Trends in Analytical Chemistry*, 116, 340–345.
37. Da Silva, K. M., Iturrospe, E., Heyrman, J., Koelmel, J. P., Cuykx, M., Vanhaecke, T., Covaci, A., & Van Nuijs, A. L. N. (2021). Optimization of a liquid chromatography-ion mobility-high resolution mass spectrometry platform for untargeted lipidomics and application to HepaRG cell extracts. *Talanta*, 235, 122808.
38. Köfeler, H. C., Eichmann, T. O., Ahrends, R., Bowden, J. A., Danne-Rasche, N., Dennis, E. A., Fedorova, M., Griffiths, W. J., Han, X., Hartler, J., Holčapek, M., Jirásko, R., Koelmel, J. P., Ejsing, C. S., Liebisch, G., Ni, Z., O'donnell, V. B., Quehenberger, O., Schwudke, D., ..., Ekroos, K. (2021). Quality control requirements for the correct annotation of lipidomics data. *Nature Communications*, 12, 4771.
39. Schrimpe-Rutledge, A. C., Codreanu, S. G., Sherrod, S. D., & Mclean, J. A. (2016). Untargeted metabolomics strategies-challenges and emerging directions. *Journal of The American Society for Mass Spectrometry*, 27, 1897–1905.
40. Zhang, C., Zuo, T., Wang, X., Wang, H., Hu, Y., Li, Z., Li, W., Jia, Li., Qian, Y., Yang, W., & Yu, H. (2019). Integration of Data-Dependent Acquisition (DDA) and Data-Independent High-Definition MSE (HDMSE) for the comprehensive profiling and characterization of multicomponents from *Panax japonicus* by UHPLC/IM-QTOF-MS. *Molecules*, 24, 2708.
41. Shah, V., Castro-Perez, J. M., McLaren, D. G., Herath, K. B., Previs, S. F., & Roddy, T. P. (2013). Enhanced data-independent analysis of lipids using ion mobility-TOFMS E to unravel quantitative and qualitative information in human plasma. *Rapid Communications in Mass Spectrometry*, 27, 2195–2200.
42. Vasilopoulou, C. G., Sulek, K., Brunner, A.-D., Meitei, N. S., Schweiger-Hufnagel, U., Meyer, S. W., Barsch, A., Mann, M., & Meier, F. (2020). Trapped ion mobility spectrometry and PASEF enable in-depth lipidomics from minimal sample amounts. *Nature Communications*, 11, 331.
43. Pezzatti, J., González-Ruiz, V., Boccad, J., Guillaume, D., & Rudaz, S. (2020). Evaluation of different tandem ms acquisition modes to support metabolite annotation in human plasma using ultra high-performance liquid chromatography high-resolution mass spectrometry for untargeted metabolomics. *Metabolites*, 10, 1–17.
44. Pettit, M. E., Brantley, M. R., Donnarumma, F., Murray, K. K., & Solouki, T. (2018). Broadband ion mobility deconvolution for rapid analysis of complex mixtures. *Analyst*, 143, 2574–2586.
45. Hellhake, S., Meckelmann, S. W., Empl, M. T., Rentmeister, K., Wißdorf, W., Steinberg, P., Schmitz, O. J., Benter, T., & Schebb, N. H. (2020). Non-targeted and targeted analysis of oxylipins in combination with charge-switch derivatization by ion mobility high-resolution mass spectrometry. *Analytical and Bioanalytical Chemistry*, 412, 5743–5757.
46. Hinz, C., Liggi, S., Mocciano, G., Jung, S., Induruwa, I., Pereira, M., Bryant, C. E., Meckelmann, S. W., O'donnell, V. B., Farndale, R. W., Fjeldsted, J., & Griffin, J. L. (2019). A comprehensive UHPLC ion mobility quadrupole time-of-flight method for profiling and quantification of eicosanoids, other oxylipins, and fatty acids. *Analytical Chemistry*, 91, 8025–8035.
47. Plachká, K., Pezzatti, J., Musenga, A., Nicoli, R., Kuuranne, T., Rudaz, S., Nováková, L., & Guillaume, D. (2021). Ion mobility-high resolution mass spectrometry in doping control analysis. Part II: Comparison of acquisition modes with and without ion mobility. *Analytica Chimica Acta*, 1175, 338739.
48. Kirkwood, K. I., Christopher, M. W., Burgess, J. L., Littau, S. R., Foster, K., Richey, K., Pratt, B. S., Shulman, N., Tamura, K., Maccoss, M. J., Maclean, B. X., & Baker, E. S. (2022). Development and application of multidimensional lipid libraries to investigate lipidomic dysregulation related to smoke inhalation injury severity. *Journal of Proteome Research*, 21, 232–242.
49. Odenkirk, M. T., Horman, B. M., Dodds, J. N., Patisaul, H. B., & Baker, E. S. (2022). Combining micropunch histology and multidimensional lipidomic measurements for in-depth tissue mapping. *ACS Measurement Science Au*, 2, 67–75.
50. Mairinger, T., Kurulugama, R., Causon, T. J., Stafford, G., Fjeldsted, J., & Hann, S. (2019). Rapid screening methods for yeast sub-metabolome analysis with a high-resolution ion mobility quadrupole time-of-flight mass spectrometer. *Rapid Communications in Mass Spectrometry*, 33, 66–74.
51. Feuerstein, M. L., Kurulugama, R. T., Hann, S., & Causon, T. (2021). Novel acquisition strategies for metabolomics using drift tube ion mobility-quadrupole resolved all ions time-of-flight mass spectrometry (IM-QRAI-TOFMS). *Analytica Chimica Acta*, 1163, 338508.
52. Picache, J. A., Rose, B. S., Balinski, A., Leaptrot, K. L., Sherrod, S. D., May, J. C., & Mclean, J. A. (2019). Collision cross section compendium to annotate and predict multi-omic compound identities. *Chemical Science*, 10, 983–993.
53. Zheng, X., Aly, N. A., Zhou, Y., Dupuis, K. T., Bilbao, A., Paurus, V. L., Orton, D. J., Wilson, R., Payne, S. H., Smith, R. D., & Baker, E. S. (2017). A structural examination and collision cross section database for over 500 metabolites and xenobiotics using drift tube ion mobility spectrometry. *Chemical Science*, 8, 7724–7736.
54. Berry, K. A. Z., Barkley, R. M., Berry, J. J., Hankin, J. A., Hoyes, E., Brown, J. M., & Murphy, R. C. (2017). Tandem mass spectrometry in combination with product ion mobility for the identification of phospholipids. *Analytical Chemistry*, 89, 916–921.



55. Hankin, J. A., Barkley, R. M., Zemski-Berry, K., Deng, Y., & Murphy, R. C. (2016). Mass spectrometric collisional activation and product ion mobility of human serum neutral lipid extracts. *Analytical Chemistry*, 88, 6274–6282.
56. Di Giovanni, J. P., Barkley, R. M., Jones, D. N. M., Hankin, J. A., & Murphy, R. C. (2018). Tandem mass spectrometry and ion mobility reveals structural insight into eicosanoid product ion formation. *Journal of The American Society for Mass Spectrometry*, 29, 1231–1241.
57. Castro-Perez, J., Roddy, T. P., Nibbering, N. M. M., Shah, V., McLaren, D. G., Previs, S., Attygalle, A. B., Herath, K., Chen, Z., Wang, S.-P., Mitnaul, L., Hubbard, B. K., Vreeken, R. J., Johns, D. G., & Hankemeier, T. (2011). Localization of fatty acyl and double bond positions in phosphatidylcholines using a dual stage CID fragmentation coupled with ion mobility mass spectrometry. *Journal of The American Society for Mass Spectrometry*, 22, 1552–1567.
58. Bouza, M., Li, Y., Wang, A. C., Wang, Z. L., & Fernández, F. M. (2021). Triboelectric nanogenerator ion mobility-mass spectrometry for in-depth lipid annotation. *Analytical Chemistry*, 93, 5468–5475.
59. Meier, F., Beck, S., Grassl, N., Lubeck, M., Park, M. A., Raether, O., & Mann, M. (2015). Parallel accumulation-serial fragmentation (PASEF): Multiplying sequencing speed and sensitivity by synchronized scans in a trapped ion mobility device. *Journal of Proteome Research*, 14, 5378–5387.
60. Meier, F., Brunner, A.-D., Koch, S., Koch, H., Lubeck, M., Krause, M., Goedecke, N., Decker, J., Kosinski, T., Park, M. A., Bache, N., Hoerning, O., Cox, J., Räther, O., & Mann, M. (2018). Online parallel accumulation-serial fragmentation (PASEF) with a novel trapped ion mobility mass spectrometer. *Molecular and Cellular Proteomics*, 17, 2534–2545.
61. Helmer, P. O., Nordhorn, I. D., Korf, A., Behrens, A., Buchholz, R., Zubeil, F., Karst, U., & Hayen, H. (2021). Complementing matrix-assisted laser desorption/ionization-mass spectrometry imaging with chromatography data for improved assignment of isobaric and isomeric phospholipids utilizing trapped ion mobility-mass spectrometry. *Analytical Chemistry*, 93, 2135–2143.
62. Meier, F., Brunner, A.-D., Frank, M., Ha, A., Bludau, I., Voytik, E., Kaspar-Schoenefeld, S., Lubeck, M., Raether, O., Bache, N., Aebersold, R., Collins, B. C., Röst, H. L., & Mann, M. (2020). diaPASEF: Parallel accumulation-serial fragmentation combined with data-independent acquisition. *Nature Methods*, 17, 1229–1236.
63. Wang, H., Wang, H., Wang, X., Xu, X., Hu, Y., Li, X., Shi, X.-J., Wang, S.-M., Liu, J., Qian, Y.-X., Gao, X.-M., Yang, W.-Z., & Guo, D.-A. (2022). A novel hybrid scan approach enabling the ion-mobility separation and the alternate data-dependent and data-independent acquisitions (HDDIDDA): Its combination with off-line two-dimensional liquid chromatography for comprehensively characterizing the multicomponents from Compound Danshen Dripping Pill. *Analytica Chimica Acta*, 1193, 339320.
64. Tötsch, K., Fjeldsted, J. C., Stow, S. M., Schmitz, O. J., & Meckelmann, S. W. (2021). Effect of Sampling rate and data pretreatment for targeted and nontargeted analysis by means of liquid chromatography coupled to drift time ion mobility quadrupole time-of-flight mass spectrometry. *Journal of The American Society for Mass Spectrometry*, 32, 2592–2603.
65. Li, T., Yin, Y., Zhou, Z., Qiu, J., Liu, W., Zhang, X., He, K., Cai, Y., & Zhu, Z.-J. (2021). Ion mobility-based sterolomics reveals spatially and temporally distinctive sterol lipids in the mouse brain. *Nature Communications*, 12, 4343.
66. Chen, Xi., Yin, Y., Zhou, Z., Li, T., & Zhu, Z.-J. (2020). Development of a combined strategy for accurate lipid structural identification and quantification in ion-mobility mass spectrometry based untargeted lipidomics. *Analytica Chimica Acta*, 1136, 115–124.
67. Zhou, Z., Luo, M., Chen, Xi., Yin, Y., Xiong, X., Wang, R., & Zhu, Z.-J. (2020). Ion mobility collision cross-section atlas for known and unknown metabolite annotation in untargeted metabolomics. *Nature Communications*, 11, 4334.
68. Dodds, J. N., & Baker, E. S. (2021). Improving the speed and selectivity of newborn screening using ion mobility spectrometry-mass spectrometry. *Analytical Chemistry*, 93, 17094–17102.
69. May, J. C., Knochenmuss, R., Fjeldsted, J. C., & Mclean, J. A. (2020). Resolution of isomeric mixtures in ion mobility using a combined demultiplexing and peak deconvolution technique. *Analytical Chemistry*, 92, 9482–9492.
70. Myllymäki, H., Astorga Johansson, J., Grados Porro, E., Elliot, A., Moses, T., & Feng, Yi. (2021). Metabolic alterations in preneoplastic development revealed by untargeted metabolomic analysis. *Frontiers in Cell and Developmental Biology*, 9, 684036.
71. Kurulugama, R. T., Darland, Ed., Kuhlmann, F., Stafford, G., & Fjeldsted, J. (2015). Evaluation of drift gas selection in complex sample analyses using a high performance drift tube ion mobility-QTOF mass spectrometer. *Analyst*, 140, 6834–6844.
72. Paglia, G., Williams, J. P., Menikarachchi, L., Thompson, J. W., Tyldesley-Worster, R., Halldórsson, S., Rolfsson, O., Moseley, A., Grant, D., Langridge, J., Pálsson, B. O., & Astarita, G. (2014). Ion mobility derived collision cross sections to support metabolomics applications. *Analytical Chemistry*, 86, 3985–3993.
73. Li, A., Conant, C. R., Zheng, X., Bloodsworth, K. J., Orton, D. J., Garimella, S. V. B., Attah, I. K., Nagy, G., Smith, R. D., & Ibrahim, Y. M. (2020). Assessing collision cross section calibration strategies for traveling wave-based ion mobility separations in structures for lossless ion manipulations. *Analytical Chemistry*, 92, 14976–14982.
74. Gabelica, V., Shvartsburg, A. A., Afonso, C., Barran, P., Benesch, J. L. P., Bleiholder, C., Bowers, M. T., Bilbao, A., Bush, M. F., Campbell, J. L., Campuzano, I. D. G., Causon, T., Clowers, B. H., Creaser, C. S., De Pauw, E., Far, J., Fernandez-Lima, F., Fjeldsted, J. C., Giles, K., ... Wyttenbach, T. (2019). Recommendations for reporting ion mobility Mass Spectrometry measurements. *Mass Spectrometry Reviews*, 38, 291–320.
75. Lee, J.-Y., Bilbao, A., Conant, C. R., Bloodsworth, K. J., Orton, D. J., Zhou, M., Wilson, J. W., Zheng, X., Webb, I. K., Li, A., Hixson, K. K., Fjeldsted, J. C., Ibrahim, Y. M., Payne, S. H., Jansson, C., Smith, R. D., & Metz, T. O. (2021). AutoCCS: Automated collision cross-section calculation software for ion mobility spectrometry-mass spectrometry. *Bioinformatics*, 37, 4193–4201.
76. May, J. C., Morris, C. B., & McLean, J. A. (2017). Ion mobility collision cross section compendium. *Analytical Chemistry*, 89, 1032–1044.
77. Hines, K. M., May, J. C., Mclean, J. A., & Xu, L. (2016). Evaluation of collision cross section calibrants for structural analysis of lipids by traveling wave ion mobility-mass spectrometry. *Analytical Chemistry*, 88, 7329–7336.
78. Ieritano, C., Lee, A., Crouse, J., Bowman, Z., Mashmouhi, N., Crossley, P. M., Friebe, B. P., Campbell, J. L., & Hopkins, W. S. (2021). Determining collision cross sections from differential ion mobility spectrometry. *Analytical Chemistry*, 93, 8937–8944.
79. Hines, K. M., Herron, J., & Xu, L. (2017). Assessment of altered lipid homeostasis by HILIC-ion mobility-mass spectrometry-based lipidomics. *Journal of Lipid Research*, 58, 809–819.
80. Ma, J., Casey, C. P., Zheng, X., Ibrahim, Y. M., Wilkins, C. S., Renslow, R. S., Thomas, D. G., Payne, S. H., Monroe, M. E., Smith, R. D., Teeguarden, J. G., Baker, E. S., & Metz, T. O. (2017). PIXIE: An algorithm for automated ion mobility arrival time extraction and collision cross section calculation using global data association. *Bioinformatics*, 33, 2715–2722.
81. Ross, D. H., Cho, J. Ho., Zhang, R., Hines, K. M., & Xu, L. (2020). LiPydomics: A python package for comprehensive prediction of lipid collision cross sections and retention times and analysis of ion mobility-mass spectrometry-based lipidomics data. *Analytical Chemistry*, 92, 14967–14975.
82. Smith, C. A., Want, E. J., O’maille, G., Abagyan, R., & Siuzdak, G. (2006). XCMS: Processing mass spectrometry data for metabolite

- profiling using nonlinear peak alignment, matching, and identification. *Analytical Chemistry*, 78, 779–787.
83. Shvartsburg, A. A., & Jarrold, M. F. (1996). An exact hard-spheres scattering model for the mobilities of polyatomic ions. *Chemical Physics Letters*, 261, 86–91.
  84. Wyttenbach, T., Von Helden, G., Batka, J. J., Carlat, D., & Bowers, M. T. (1997). Effect of the long-range potential on ion mobility measurements. *Journal of The American Society for Mass Spectrometry*, 8, 275–282.
  85. Bleiholder, C., Wyttenbach, T., & Bowers, M. T. (2011). A novel projection approximation algorithm for the fast and accurate computation of molecular collision cross sections (I). *Method. International Journal of Mass Spectrometry*, 308, 1–10.
  86. Marklund, E. G., Degiacomi, M. T., Robinson, C. v., Baldwin, A. J., & Benesch, J. L. P. (2015). Collision cross sections for structural proteomics. *Structure*, 23, 791–799.
  87. Paizs, B. (2015). A divide-and-conquer approach to compute collision cross sections in the projection approximation method. *International Journal of Mass Spectrometry*, 378, 360–363.
  88. Ewing, S. A., Donor, M. T., Wilson, J. W., & Prell, J. S. (2017). Colli-doscope: An improved tool for computing collisional cross-sections with the trajectory method. *Journal of The American Society for Mass Spectrometry*, 28, 587–596.
  89. Colby, S. M., Thomas, D. G., Nuñez, J. R., Baxter, D. J., Glaesemann, K. R., Brown, J. M., Pirrung, M. A., Govind, N., Teegarden, J. G., Metz, T. O., & Renslow, R. S. (2019). ISiCLE: A quantum chemistry pipeline for establishing in silico collision cross section libraries. *Analytical Chemistry*, 91, 4346–4356.
  90. Zannotto, L., Heerd, G., Souza, P. C. T., Araujo, G., & Skaf, M. S. (2018). High performance collision cross section calculation-HPPCS. *Journal of Computational Chemistry*, 39, 1675–1681.
  91. Zhou, Z., Xiong, X., & Zhu, Z.- J. (2017). MetCCS predictor: A web server for predicting collision cross-section values of metabolites in ion mobility-mass spectrometry based metabolomics. *Bioinformatics*, 33, 2235–2237.
  92. Zhou, Z., Tu, J., Xiong, X., Shen, X., & Zhu, Z. J. (2017). LipidCCS: Prediction of collision cross-section values for lipids with high precision to support ion mobility-mass spectrometry-based lipidomics. *Analytical Chemistry*, 89, 9559–9566.
  93. Plante, P.- L., Francovic-Fontaine, É., May, J. C., Mclean, J. A., Baker, E. S., Laviolette, F., Marchand, M., & Corbeil, J. (2019). Predicting ion mobility collision cross-sections using a deep neural network: DeepCCS. *Analytical Chemistry*, 91, 5191–5199.
  94. Ross, D. H., Cho, J. Ho., & Xu, L. (2020). Breaking down structural diversity for comprehensive prediction of ion-neutral collision cross sections. *Analytical Chemistry*, 92, 4548–4557.
  95. Colby, S. M., Nuñez, J. R., Hodas, N. O., Corley, C. D., & Renslow, R. R. (2019). Deep learning to generate in silico chemical property libraries and candidate molecules for small molecule identification in complex samples. *Analytical Chemistry*, 92, 1720–1729.
  96. Laphorn, C., Pullen, F. S., Chowdhry, B. Z., Wright, P., Perkins, G. L., & Heredia, Y. (2015). How useful is molecular modelling in combination with ion mobility mass spectrometry for “small molecule” ion mobility collision cross-sections? *Analyst*, 140, 6814–6823.
  97. Soper-Hopper, M. T., Petrov, A. S., Howard, J. N., Yu, S. S., Forsythe, J. G., Grover, M. A., & Fernández, F. M. (2017). Collision cross section predictions using 2-dimensional molecular descriptors. *Chemical Communications*, 53, 7624–7627.
  98. Mollerup, C. B., Mardal, M., Dalsgaard, P. W., Linnet, K., & Barron, L. P. (2018). Prediction of collision cross section and retention time for broad scope screening in gradient reversed-phase liquid chromatography-ion mobility-high resolution accurate mass spectrometry. *Journal of Chromatography A*, 1542, 82–88.
  99. Bijlsma, L., Bade, R., Celma, A., Mullin, L., Cleland, G., Stead, S., Hernandez, F., & Sancho, J. V. (2017). Prediction of collision cross-section values for small molecules: Application to pesticide residue analysis. *Analytical Chemistry*, 89, 6583–6589.
  100. Wishart, D. S., Guo, A., Oler, E., Wang, F., Anjum, A., Peters, H., Dizon, R., Sayeeda, Z., Tian, S., Lee, B. L., Berjanskii, M., Mah, R., Yamamoto, M., Jovel, J., Torres-Calzada, C., Hiebert-Giesbrecht, M., Lui, V. W., Varshavi, D., Varshavi, D., ..., Gautam, V., HMDB 5.0: The human metabolome database for 2022 (2022). *Nucleic Acids Research*, 50, D622–D631.
  101. Kyle, J. E., Zhang, X., Weitz, K. K., Monroe, M. E., Ibrahim, Y. M., Moore, R. J., Cha, J., Sun, X., Lovelace, E. S., Wagoner, J., Polyak, S. J., Metz, T. O., Dey, S. K., Smith, R. D., Burnum-Johnson, K. E., & Baker, E. S. (2016). Uncovering biologically significant lipid isomers with liquid chromatography, ion mobility spectrometry and mass spectrometry. *Analyst*, 141, 1649–1659.
  102. Tu, J., Zhou, Z., Li, T., & Zhu, Z.- J. (2019). The emerging role of ion mobility-mass spectrometry in lipidomics to facilitate lipid separation and identification. *TrAC - Trends in Analytical Chemistry*, 116, 332–339.
  103. Kliman, M., May, J. C., & Mclean, J. A. (2011). Lipid analysis and lipidomics by structurally selective ion mobility-mass spectrometry. *Biochimica et Biophysica Acta - Molecular and Cell Biology of Lipids*, 1811, 935–945.
  104. Kim, H. I., Kim, H., Pang, E. S., Ryu, E. K., Beegle, L. W., Loo, J. A., Goddard, W. A., & Kanik, I. (2009). Structural characterization of unsaturated phosphatidylcholines using traveling wave ion mobility spectrometry. *Analytical Chemistry*, 81, 8289–8297.
  105. Tsugawa, H., Ikeda, K., Takahashi, M., Satoh, A., Mori, Y., Uchino, H., Okahashi, N., Yamada, Y., Tada, I., Bonini, P., Higashi, Y., Okazaki, Y., Zhou, Z., Zhu, Z.- J., Koelmel, J., Cajka, T., Fiehn, O., Saito, K., Arita, M., & Arita, M. (2020). A lipidome atlas in MS-DIAL 4. *Nature Biotechnology*, 38, 1159–1163.
  106. Picache, J. A., May, J. C., & Mclean, J. A. (2020). Chemical class prediction of unknown biomolecules using ion mobility-mass spectrometry and machine learning: Supervised inference of feature taxonomy from ensemble randomization. *Analytical Chemistry*, 92, 10759–10767.
  107. Adams, K. J., Pratt, B., Bose, N., Dubois, L. G., St John-Williams, L., Perrott, K. M., Ky, K., Kapahi, P., Sharma, V., Maccoss, M. J., Moseley, M. A., Colton, C. A., Maclean, B. X., Schilling, B., & Thompson, J. W. (2020). Skyline for small molecules: A unifying software package for quantitative metabolomics. *Journal of Proteome Research*, 19, 1447–1458.
  108. Gil-De-La-Fuente, A., Godzien, J., Saugar, S., Garcia-Carmona, R., Badran, H., Wishart, D. S., Barbas, C., & Otero, A. (2019). CEU mass mediator 3.0: A metabolite annotation tool. *Journal of Proteome Research*, 18, 797–802.
  109. Koomen, D. C., May, J. C., & Mclean, J. A. (2022). Insights and prospects for ion mobility-mass spectrometry in clinical chemistry. *Expert Review of Proteomics*, 19, 17–31.

**How to cite this article:** Moran-Garrido, M., Camunas-Alberca, S. M., Gil-de-la Fuente, A., Mariscal, A., Gradillas, A., Barbas, C., & Sáiz, J. (2022). Recent developments in data acquisition, treatment and analysis with ion mobility-mass spectrometry for lipidomics. *Proteomics*, 22, e2100328. <https://doi.org/10.1002/pmic.202100328>